Characterising changes in adhesion and enzyme activity related to drug resistance in colon cancer cells

by

Heather Nicole Dekker

A thesis

presented to the University of Waterloo

in fulfilment of the

thesis requirement for the degree of

Master of Science

in

Pharmacy

Waterloo, Ontario, Canada, 2018

Author's Declaration

I hereby declare that I am the sole author of this thesis. This is a true copy of the thesis, including any required final revisions, as accepted by my examiners.

I understand that my thesis may be made electronically available to the public.

Abstract

Metastatic colorectal cancer is often fatal, and drug resistance to chemotherapeutic agents is one of the primary contributing factors to this lethality. Drug resistance arises from exposure to chemotherapies, and it can be mediated through a variety of mechanisms. One of these mechanisms is alteration of enzymes within the cancer cells to affect the processing or removal of the drug. Carboxylesterase is an example of an enzyme that converts irinotecan, a drug used in metastatic colorectal cancer treatments, into the active metabolite SN-38. Carboxylesterase enzymes are found in high quantities in both the liver and intestinal cells. The presence of carboxylesterase in intestinal and liver cells is an important consideration in the processing of colorectal cancer treatments. Glutathione S-transferase is another enzyme that has been implicated in drug resistance because of its ability to conjugate reduced glutathione to xenobiotic substances, facilitating their removal. Additionally, drug resistance can affect the behaviours of cells. Drug-resistant cells can exhibit changes in their motility and aggressiveness compared to drug-sensitive cells. In this study I investigated cellular behavioural changes in SN-38-resistant colon cancer cells compared to their SN-38-sensitive counterparts. In addition to behavioural changes, I also sought to determine if elevations in carboxylesterase and glutathione S-transferase enzymes were contributing to the drug resistance in these colon cancer cells.

Acknowledgements

I wish to thank my supervisor, Dr. Jonathan Blay, for his continued support and understanding as I completed my Masters degree. He always had either a humorous perspective or sage insight to share. I am also deeply thankful for the liveliness and depth of discussion provided by my advisory committee members, Dr. Tejal Patel and Dr. Mungo Marsden, throughout the duration of my studies.

I am thankful to my lab mates – Alex, Deep, Bogdan, Julia, Hayden, and Spencer – for being there to trouble-shoot, bounce ideas, go out for meals, or engage in political and philosophical discussions with.

To my parents, Florence and George, I would like to say thank you for the continued support throughout all of my academic endeavours. All the way from my childhood hand-held microscope, to present day conversations regarding where I am off to next. You continually fuelled my inquisitive mind, for which I am truly grateful. As for my siblings, thank you for adding support and variety to my life, even as we have all headed in different directions (quite literally across the country and even the world at times).

Finally, I would like to thank my family – Paul, Florence, and Astrid – for persisting with me through the ups and downs of lab work, the continuum of writing, and the practicing of presentations. Nothing works quite like the reading of a thesis or presentation to put children to sleep (ahem, Florence). I would especially like to thank Paul for contending with a wife who not only was riding through the trials of a degree, but one who was pregnant for the majority of the time doing so.

Table of Contents

Author's Declaration ii

Abstract iii

Acknowledgements iv

List of Figures viii

List of Tables ix

List of Abbreviations x

Chapter 1. Introduction 1

1.1 Colorectal Cancer Overview 1

1.1.1 Colorectal cancer 1

1.1.2 Common mutations in colorectal cancer 2

1.1.3 Progression and stages of colorectal cancer 2

1.2 Colorectal Cancer Treatments 5

1.3 Drug Metabolism 8

1.4 Drug Resistance in Colorectal Cancer 10

1.4.1 Overview of drug resistance 10

1.4.2 Heterogeneity of cancer and drug resistance 11

1.4.3 Altered cell cycle checkpoints and repair mechanisms 13

1.4.4 Alteration of drug targets and metabolic changes in drug resistance 13

1.4.5 Cell signalling changes in drug resistance 14

1.4.6 Altered uptake and efflux of compounds in drug-resistant cancer 14

1.5 Altered Behaviours of Drug-Resistant Cells 15

1.6 Cell Adhesion 16

1.7 Carboxylesterase 17

1.8 Glutathione S-Transferase 18

1.9 Rationale for the Project 19

1.10 Hypothesis and Objectives 20

Chapter 2. Methods 21

2.1 Cell Culture 21

2.2 Staining Cells with 5-chloromethylfluorescein diacetate (CMFDA) 22

2.3 Cell Adhesion Assays 23

2.3.1 Cell adhesion assays on glass coverslips 23
2.3.2 Cell adhesion on a fibronectin substratum 24
2.3.3 Cell adhesion on a HepG2 hepatocellular carcinoma monolayer 25
2.4 5-chloromethylfluorescein diacetate (CMFDA) Conversion Experiment 26
2.5 Carboxylesterase Activity Assays 27
2.5.1 4-methylumbelliferyl acetate (4-MUBA) conversion 27
2.5.2 p-nitrophenyl acetate (pNP) conversion 31
2.6 Glutathione S-Transferase Activity Assay 35
2.7 Statistical Analysis 39
2.8 Generation of Figures 39
Chapter 3. Results 40
3.1 Cell Adhesion 40
3.1.1 Overview 40
3.1.2 Adhesion of HT29 and SN-38-resistant HT29-S cells to fibronectin 40
3.1.3 Adhesion of HT29 and SN-38-resistant HT29-S cells to HepG2 hepatocellular carcinoma cells 42
3.2 5-chloromethylfluorescein diacetate (CMFDA) Conversion in Colon Cancer Cells 45
3.3 Carboxylesterase 48
3.3.1 4-methylumbelliferyl acetate (4-MUBA) conversion in colon cancer cells 48
3.3.2 p-nitrophenyl acetate (pNP) conversion in colon cancer cells 50
3.4 Glutathione S-Transferase 52
Chapter 4. Discussion 55
4.1 Perspective 55
4.2 Cell Adhesion 56
4.3 5-chloromethylfluorescein diacetate (CMFDA) 58
4.4 Carboxylesterase 61
4.4.1 Overview 61
4.4.2 4-methyumbelliferyl acetate (4-MUBA) conversion in SN-38-resistant colon cancer cells 62
4.4.3 p-nitrophenyl acetate (pNP) conversion in SN-38-resistant colon cancer cells 63
4.4.4 Importance of carboxylesterase activity in drug resistance 64
4.4.5 Clinical relevance of carboxylesterase in colorectal cancer 65

4.5 Glutathione S-Transferase 66
4.5.1 Overview 66
4.5.2 Glutathione S-transferase involvement in cell survival 68
4.5.3 Clinical considerations of glutathione S-transferase in cancer treatment 71
4.6 Limitations of this Work 72
4.7 Significance of this Work 73
References 74
Appendix 78
A.1 Buffer and Reagent Recipes 78
A.1.1 Phosphate Buffered Saline 78
A.1.2 Paraformaldehyde 78
A.1.3 Lysis Buffer 78
A.1.4 Phosphate Buffer with Ca^{2+} Mg^{2+} 78

List of Figures

Figure 1 Stages 0 to 4 of colorectal cancer 3
Figure 2 Structures of chemotherapy drugs 6
Figure 3 Metabolic pathway of irinotecan in the liver 9
Figure 4 Mechanisms of drug resistance in cells 12
Figure 5 Time course of carboxylesterase activity in colon cancer cells using 4-methylumbelliferyl acetate 28
Figure 6 Fluorescence of clear and black 96-well plates and solutions used in 4-methylumbelliferyl acetate experiments 30
Figure 7 Cytotoxicity of 2.0 mM p-nitrophenyl acetate in different colon cancer cells 32
Figure 8 Conversion of p-nitrophenyl acetate in different colon cancer cells 34
Figure 9 Glutathione S-transferase activity in different colon cancer cells 37
Figure 10 Increased adhesion of SN-38-resistant HT29-S colon cancer cells to fibronectin 41
Figure 11 HT29 colon cancer cells adhered to a HepG2 hepatocellular carcinoma monolayer 43
Figure 12 Increased adhesion of SN-38-resistant HT29-S colon cancer cells on a HepG2 hepatocellular carcinoma monolayer 44
Figure 13 5-chloromethylfluorescein diacetate (CMFDA) conversion in different colon cancer cells 46
Figure 14 Carboxylesterase activity in different colon cancer cells using 4-methyumbelliferyl acetate (4-MUBA) 49
Figure 15 Carboxylesterase activity in different colon cancer cells using p-nitrophenyl acetate (pNP) 51
Figure 16 Glutathione S-transferase activity in different colon cancer cells using 1-chloro-2,4-dinitrobenzene (CDNB) and reduced glutathione (GSH) 53
Figure 17 5-chloromethylfluorescein (CMFDA) conversion within a cell 59
Figure 18 GSTP1 inhibition of JNK1 69

List of Tables

Table 1 Cell lines and cell culture components 21
Table 2 Solution volumes for glutathione S-transferase activity experiments using 1 mM 1-chloro-2,4-dinitrobenzene (CDNB) and 2 mM reduced glutathione (GSH) 36
Table 3 Solution volumes for glutathione S-transferase activity experiments using six concentrations of 1-chloro-2,4-dinitrobenzene (CDNB) and reduced glutathione (GSH) 38

List of Abbreviations

4-MUBA	4-methylumbelliferyl acetate
5-FU	5-Fluorouracil
ABC	ATP binding cassette
APC	Adenomatous polyposis coli
BSA	Bovine serum albumin
CDNB	1-chloro-2,4-dinitrobenzene
CES	Carboxylesterase
CES1	Carboxylesterase 1
CES2	Carboxylesterase 2
CMFDA	5-chloromethylfluorescein diacetate
CRC	Colorectal cancer
CYP	Cytochrome P450
DAPI	2-(4-amidinophenyl)-1H-indole-6-carboxamidine
DMEM	Dulbecco's modified Eagle's medium
ECM	Extracellular matrix
EDTA	Ethylenediaminetetraacetic acid
EMT	Epithelial to mesenchymal transition
ERK	Extracellular signal-regulated kinases
FN	Fibronectin
GSH	Reduced glutathione
GST	Glutathione S-transferase
GSTP	Glutathione S-transferase pi
JNK	c-Jun N-terminal kinase
MAPK	Mitogen activating protein kinase
MET	Mesenchymal to epithelial transition
PBS	Phosphate buffered saline
PFA	Paraformaldehyde
PLL	Poly-L-lysine
P-gp	P-glycoprotein
pNP	p-nitrophenyl acetate
RGD	Arginine-glycine-aspartic acid
SEM	Standard error of the mean
SN-38	7-ethyl-10-hydroxycamptothecin
SN-38G	7-ethyl-10-hydroxycamptothecin glucuronide
UGT	UDP glucuronosyl transferase

Chapter 1. Introduction

1.1 Colorectal Cancer Overview

1.1.1 Colorectal cancer

Colorectal cancer (CRC) is the third most common cancer in the world, and the second most common in Canada; affecting one in thirteen men and one in sixteen women (Cancer Stats 2017). CRC arises from normal cells after they accumulate a series of common mutations in important genes. These mutations often result in altered oncogenes and loss of tumour suppressor gene function, contributing to the progression of CRC [1-3]. Some of the primary genes involved in this change are the adenomatous polyposis coli (APC) gene [4], K-*ras* mutation [2, 5], transforming growth factor β [6], and p53 [5, 7]. The alteration of these genes generally leads to a loss of function or control of cell cycling, which in turn allows cells to proliferate. Some of the changes enable the cells to move beyond their normal growth checkpoints and boundaries that restrict the growth and movement of the cells.

1.1.2 Common mutations in colorectal cancer

The APC gene is considered a tumour suppressor gene, and its gene product prevents uncontrolled growth of cells. An APC gene mutation can be congenital and result from an inherited mutation causing familial adenomatous polyposis. This hereditary mutation predisposes people to CRC because they have a higher rate of polyp production compared to normal [8]. An APC mutation is often one of the first steps in a series of mutations that initiate CRC development [9].

One of the most commonly mutated genes, found in roughly 40% of CRC cases, is a deleted or altered KRAS [2]. Many KRAS mutations result in constitutively active K-*ras* protein which maintains proliferation and survival signals. Another protein that is often changed in CRC is p53. p53 is a cellular checkpoint protein that prevents cells from continuing to grow and divide if they have excessive DNA damage. p53 is also used by cells to shunt damaged cells towards programmed cell death, called apoptosis.

1.1.3 Progression and stages of colorectal cancer

As CRC tumour growth progresses through more layers of tissue, it is classified into stages 0 through 4 (Figure 1). The survival of a patient is closely tied to the stage of CRC they are diagnosed with. Five-year survival rates are around 90% for localised, stage 1 CRC. This high rate of survival is largely due to the successful resection of these tumours, removing the cancer. The five-year survival rates plummet to 12.5% for patients with metastatic disease [10]. Late stage cancer is challenging to treat; it is often resistant to chemotherapeutic drugs, and surgery is complicated because the cancer has spread to other areas in the body [10].

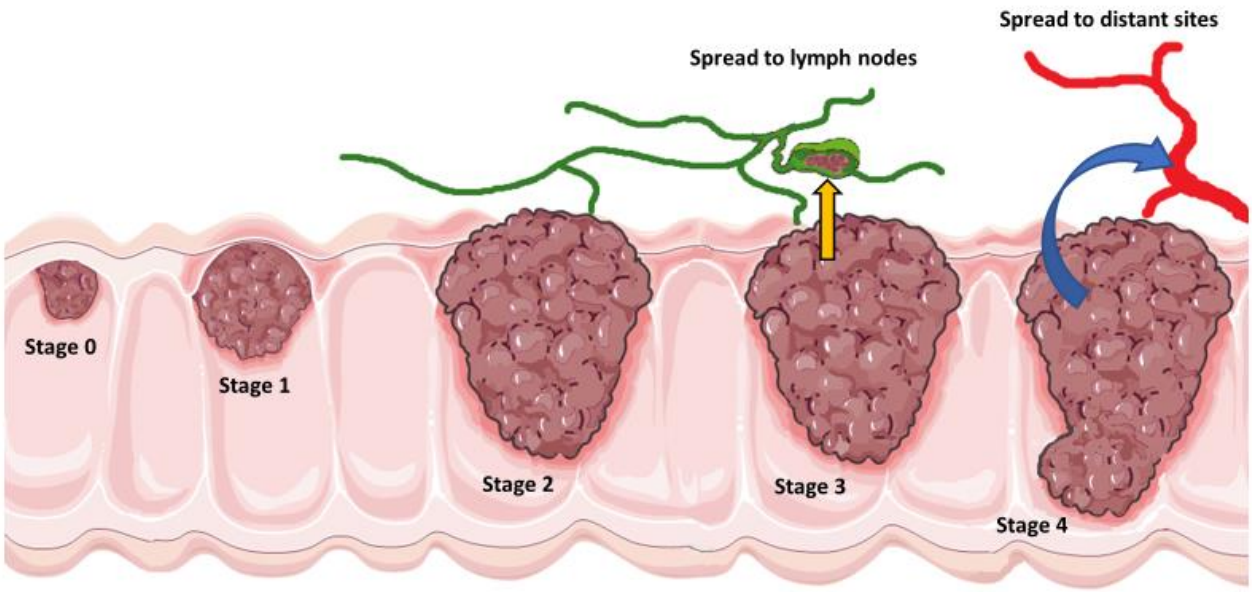

Figure 1 Stages 0 to 4 of colorectal cancer

Progression of colorectal cancer from stage 0 to stage 4 with invasion of tissue layers. Stage 0 is localised to the mucosa, stage 1 has penetrated the mucosa and submucosa. Stage 2 has progressed into the remaining two layers of tissue – the muscularis and serosa. Stage 3 CRC has migrated (yellow arrow) to nearby lymph nodes and stage 4 has spread to distant organs through the vasculature (blue arrow).

Stage 0 CRC shows the preliminary signs of change and problems associated with the tissue. In this stage, the cancer is localised and has not grown beyond the mucosa, the innermost layer of the colon. This is referred to as a carcinoma *in situ*. In stage 1 CRC, the cancer has grown into the submucosa – the connective tissue layer surrounding the mucosa. Stage 2 CRC is characterised by the carcinoma having grown into the next layers of tissue, the muscularis and serosa. In order to progress to Stage 3, the carcinoma must spread to local lymph nodes in the rectum and colon [11].

Stage 4 CRC has spread to distant organs in the body, a process called metastasis. Cancer metastasis occurs when the carcinoma breaks beyond its normal boundaries and away from the basement membrane; the cancerous cells lose their attachments to the extracellular matrix (ECM) and spread to surrounding tissues. Common sites of CRC metastasis are the liver, lungs, and brain. The liver and intestines are connected through the portal vein, which acts as a direct shunt to the liver. This physical connection contributes to the high levels of liver metastases from CRC [12]. In addition to this physical shunt, the liver likely has an appropriate niche microenvironment to attract and host circulating CRC cells [13, 14].

In order for the cancer to progress in metastasis, the cells must undergo changes that promote motility, durability, and survival of the cell while losing its constraints that keep it at the basement membrane [15]. The combination of these alterations makes the epithelial cells resemble mesenchymal cells in morphology and behaviour. These cellular changes are known as epithelial to mesenchymal transition (EMT).

1.2 Colorectal Cancer Treatments

The treatment of CRC varies depending on the stage and aggression of the disease. Stage 0 CRC can be removed using routine procedures, such as a colonoscopy, to perform a polypectomy. Typically, localised stage 1 cancer is resected along with a piece of the bowel and several nearby lymph nodes [11]. For stages 2 and 3, surgery is still considered the primary treatment for colon cancer. Adjuvant chemotherapy may be introduced for stage 2 colon cancer patients following surgery, but it is commonly given to stage 3 cancer patients. The chemotherapy drugs used often include a regimen of 5-fluorouracil (5-FU; Figure 2A), capecitabine, leucovorin, and oxaliplatin (Figure 2B) in various combinations [11, 16]. Irinotecan (Figure 2C) is introduced as a stage 4 metastatic cancer treatment and in cases of recurrent CRC. The most common combination of drugs in this late-stage scenario is FOLFIRI, which consists of leucovorin, 5-FU, and irinotecan [11].

The cytotoxic effects of these drugs are mediated through a variety of mechanisms. 5-FU – a primary component in most CRC chemotherapy treatments – is an analogue of uracil, and is transported and introduced into RNA much like uracil itself [17]. Through the integration into RNA, 5-FU and its metabolites disrupt RNA processes. 5-FU also functions as a thymidylate synthase inhibitor [17], and prevents the synthesis of deoxythymidine monophosphate which then results in lower deoxythymidine triphosphate levels downstream. The reduction in thymidine generation has detrimental effects on DNA replication because thymidine is an important deoxynucleotide; the ensuing imbalance in deoxynucleotides within the cells stimulates a variety of feedback loops and results in DNA damage [18].

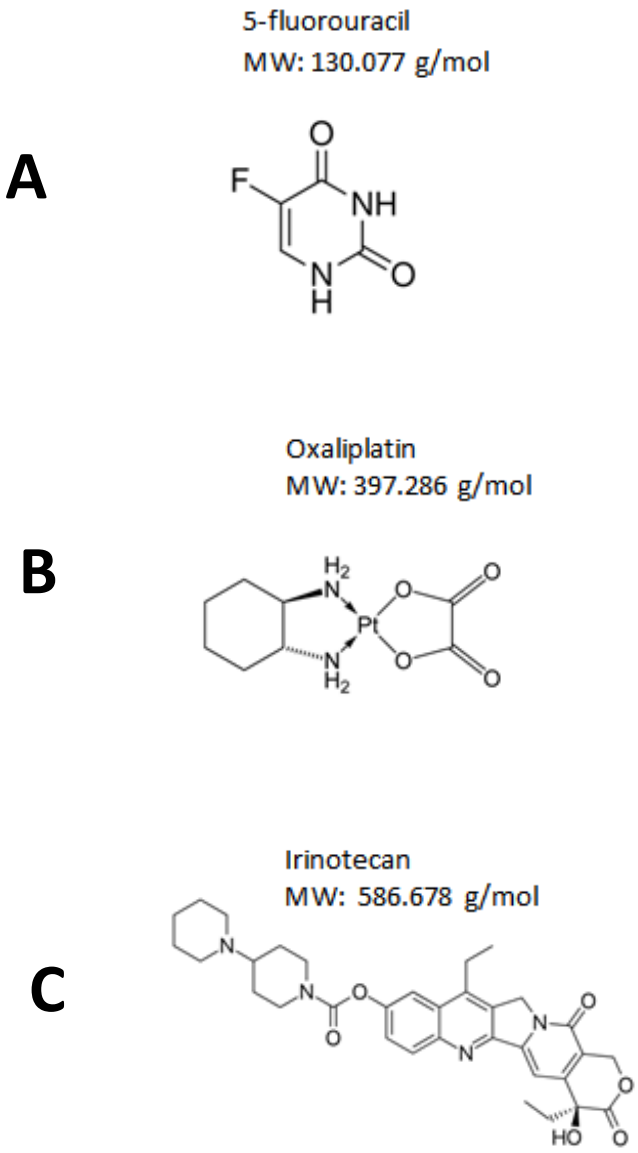

Figure 2 Structures of chemotherapy drugs

Structures and molecular weights of the chemotherapy drugs 5-fluorouracil (A), oxaliplatin (B), and irinotecan (C).

Irinotecan is reserved for advanced stage and metastatic cancer; it is a topoisomerase 1 inhibitor. This inhibition is believed to occur through the stabilisation of topoisomerase 1-DNA intermediates known as cleavable complexes. This stabilisation and inhibition of topoisomerase 1 prevents the DNA strand breaks formed during replication from being repaired. As a result, the damage impedes DNA synthesis from progressing and mitosis is halted [19].

1.3 Drug Metabolism

Many drugs are administered in a pro-drug form that must be metabolised into active metabolites. Irinotecan is a pro-drug that requires carboxylesterase (CES) enzymes to convert it into the active metabolite 7-ethyl-10-hydroxycamptothecin (SN-38) [20]. Activation of irinotecan occurs via a hydrolysis reaction involving CES cleavage of an acetate group from irinotecan, generating the SN-38 metabolite. Inactivation of SN-38 primarily occurs through a glucuronidation reaction in which glucuronic acid is conjugated to SN-38, transforming it into SN-38 glucuronide (SN-38G). SN-38G is secreted into bile for excretion [21]. Irinotecan is administered intravenously and is metabolised into its more potent active metabolite SN-38 mainly in the liver (Figure 3). The cytochrome P450 (CYP) enzyme family has prominent involvement in drug metabolism. CYP 3A4 converts irinotecan into inactive metabolites through oxidation reactions.

Irinotecan and SN-38 exist in inactive carboxylate and active lactone forms; this equilibrium is affected by pH and the presence of binding proteins [22, 23]. Lactone forms are more stable in the presence of albumin [24].

Drugs that are orally administered must pass through a variety of pH environments, and must also be able to be absorbed through the gut and into the bloodstream [25], transport of the drug to the liver can then occur following absorption in the gut.

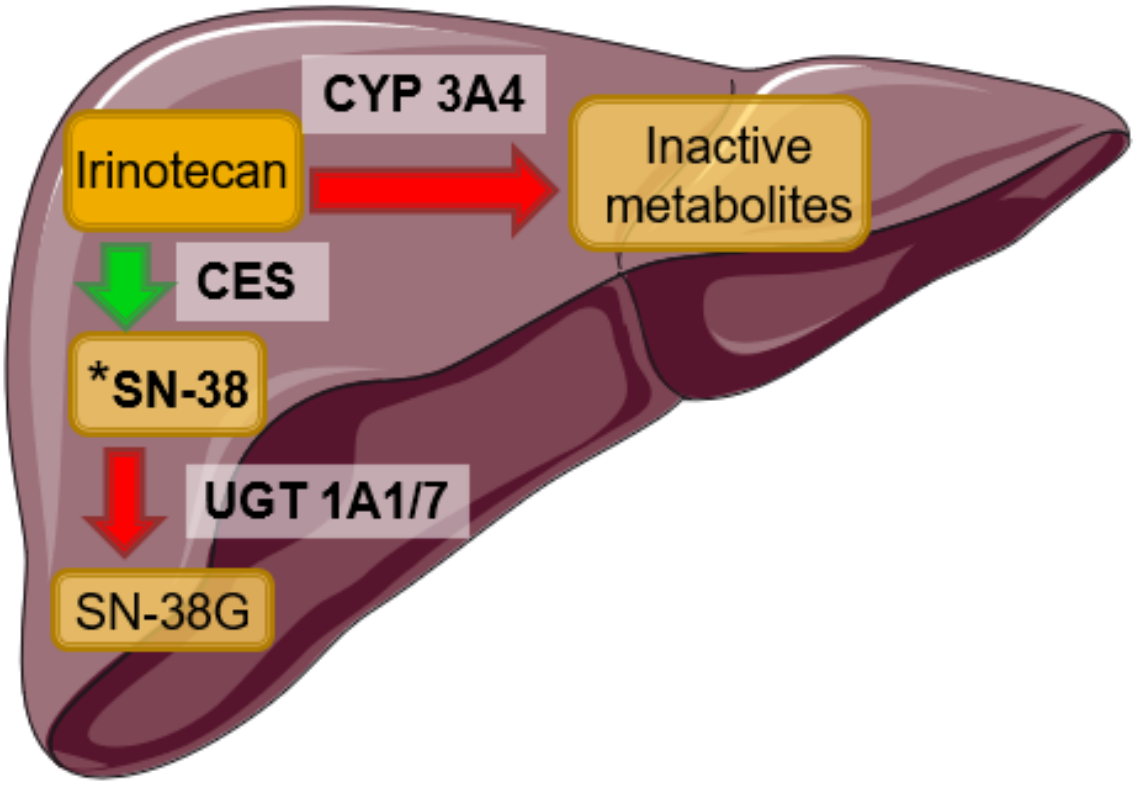

Figure 3 Metabolic pathway of irinotecan in the liver

Irinotecan is converted into the active metabolite SN-38 by carboxylesterase (CES) enzymes. SN-38 is inactivated by UDP glucuronosyltransferase (UGT) 1A1/7 enzymes, forming SN-38G. Irinotecan can be directly inactivated by cytochrome P450 3A4 (CYP 3A4) enzymes through an oxidation reaction.

1.4 Drug Resistance in Colorectal Cancer

1.4.1 Overview of drug resistance

There are two main types of drug resistance, intrinsic and acquired. Intrinsic resistance exists within the cancer prior to any treatments being administered. Acquired drug resistance occurs over the course of successive chemotherapy treatments, and is commonly found in metastatic and recurrent disease. Nearly all recurrent CRC has some form of drug resistance [26, 27]. Cells that are drug resistant are often multi-drug resistant, in which the cancer is resistant to many of the chemotherapeutic drugs used [26].

1.4.2 Heterogeneity of cancer and drug resistance

Drug resistance often arises over the course of successive chemotherapy treatments. Metastatic CRC [28] and recurrent cancers are often drug resistant because they have had exposure to successive treatments of chemotherapies. This exposure to a cytotoxic assault puts selective pressure on the cancer cells and eliminates cells unable to cope with the assault. The cells react to the flux in selective pressure by adapting to their environments and altering how they process or remove compounds [26]. These adaptations can result in drug resistance [29] through a variety of mechanisms, as indicated in Figure 4. Cells that have mechanisms to survive can then flourish.

The heterogeneity of cancer cells encourages the acquisition of resistance mechanisms and aggressive traits in the cancer [30]. The cells most able to survive the changing conditions and rigors of movement through the body are the ones that grow and repopulate. These resistance and genetic profiles of the cancer cells can change with treatments as the cells adapt to the new selective pressures they are exposed to. This adaptation has been observed in liver metastases over the course of varied treatments [31].

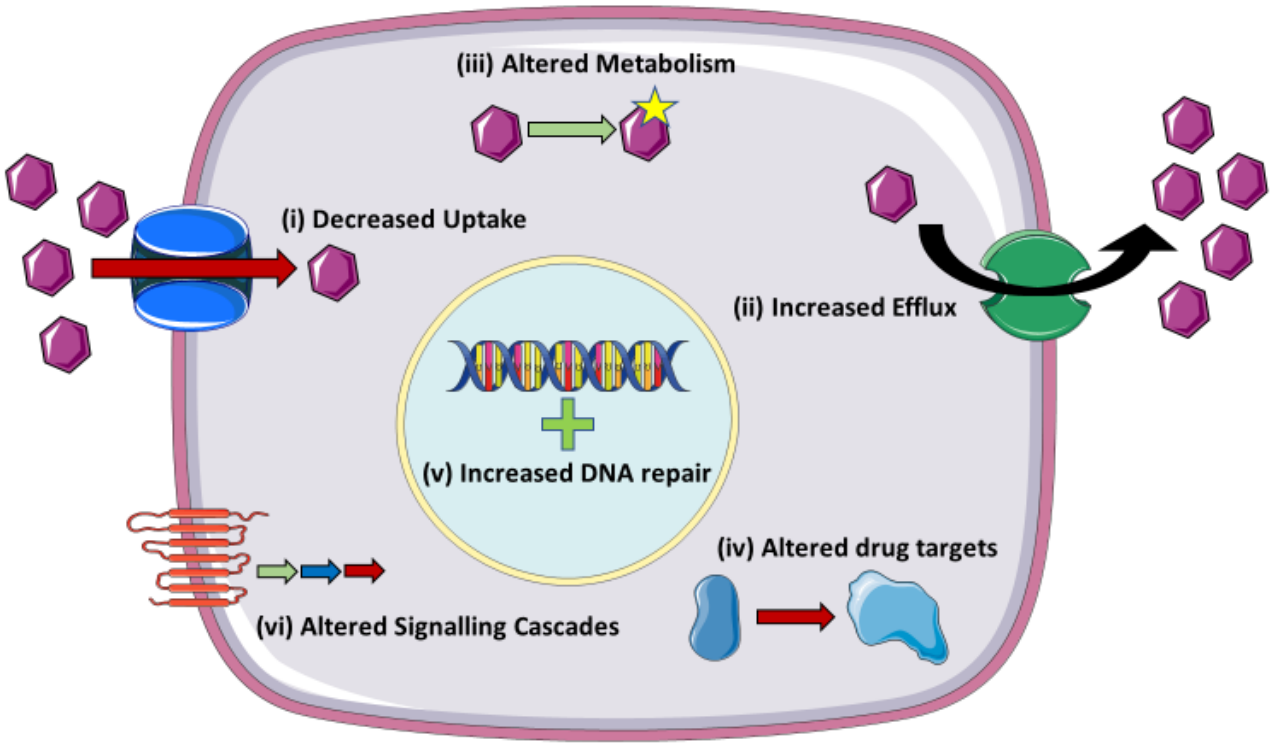

Figure 4 Mechanisms of drug resistance in cells

Potential drug resistance mechanisms that cells can employ to reduce the presence and activity of chemotherapies within the cell. Cells can decrease drug uptake (i) or increase efflux (ii) to reduce intracellular concentrations of the drug. The metabolism of the drug may be altered (iii) through decreasing activation, or increasing deactivation to render the drug inactive. Drug targets can be changed (iv) so the drugs cannot bind or act properly, limiting the cellular response to the drug. Repair of DNA can be increased (v) which limits apoptotic pathway stimulus. Finally, cellular signaling can altered (vi) to increase survival and proliferation of the cell.

1.4.3 Altered cell cycle checkpoints and repair mechanisms

Somatic cells have repair mechanisms to fix damaged DNA and remove aberrant proteins. If these repair mechanisms fail, there are checkpoints within the cell cycle to prevent progression until the problem is fixed. When the damage is too great, the cells may be triggered into apoptosis in order to eliminate the damaged and defective cells. In many cancers, these repair functions and checkpoints are often bypassed or hijacked, allowing cells to grow and proliferate without hindrance. An example of altered checkpoints would be the earlier stated mutations in p53 [7].

1.4.4 Alteration of drug targets and metabolic changes in drug resistance

The alteration of drug targets and enzymes involved in the metabolic pathways of the drugs can promote drug resistance in cells (Figure 4). Cells can lower the levels of active metabolites of drugs within the cells, and can do so through changes in the metabolism of drugs and their metabolites. These changes can be an increase deactivation or decrease activation, both of which would result in lower levels of the active metabolites being present within cells [32]. The metabolic state can also affect drug resistance in cells. A particular example of this was in lung cancer cell lines that had high levels of mitochondrial reactive oxygen species following prolonged treatment with gefitinib. These lung cancer cells exhibited EMT phenotypes until the withdrawal of gefitinib, which then led to lower levels of reactive oxygen species and a return to normal EMT markers [33].

1.4.5 Cell signalling changes in drug resistance

Alterations in cell signalling pathways are often present in cancers. The mitogen-activated protein kinase (MAPK)/extracellular signal-regulated kinases (ERK) pathway is implicated in many different cancers [34] and CRC in particular [2]. This pathway can engender carcinogenesis as well as mediate drug resistance mechanisms [35]. A cell can also decrease its response to apoptotic signals, or increase cell survival signals. These signalling changes can be accomplished by affecting the signalling molecules found within the pathways. For example, c-Jun N-terminal kinase (JNK) apoptotic signalling involves the activation of JNK1, which initiates a further signalling cascade involving pro-apoptotic Bcl-2 family proteins and caspases to stimulate cell death. An example of drug resistance involving anti-apoptotic proteins from the Bcl-2 family was demonstrated in HCT116 cells that had drug resistance mediated through overexpression of Bcl-2 family proteins, thereby decreasing apoptotic signalling and resulting in cell survival [36].

1.4.6 Altered uptake and efflux of compounds in drug-resistant cancer

Alteration of cellular excretion of unwanted compounds plays a major role in drug resistance; a cell is more likely to survive if it is capable of removing cytotoxic compounds. ATP-binding cassette (ABC) transporters actively use the catabolism of ATP to power the removal of substances from cells, and are often involved in multi-drug resistance [37]. P-glycoprotein (P-gp) is a prime example of this function of ABC transporters. P-gp is a promiscuous pump that has many interactions and the ability to remove a variety of substances and xenobiotics from the cell [38]. Increased activity of efflux pumps within cells is a large contributor to some forms of drug resistance [39].

1.5 Altered Behaviours of Drug-Resistant Cells

Drug-resistant cells often display altered aggressiveness, motility, and invasive properties [40]. Resistant cells can exhibit elongated fibroblast-like shapes, reminiscent of a mesenchymal phenotype [41]. Mesenchymal markers such as vimentin and the transcription factor Snail are often present in drug-resistant phenotypes [41, 42].

These alterations in morphology and cellular markers indicate that those drug-resistant cancers are exhibiting signs of EMT, which in turn promotes motility and survival within the body and outside the normal bounds of the tissue [43, 44]. The transformation from epithelial characteristics to mesenchymal is also indicative of progression to a stem-cell like state. The EMT and stem-cell like properties relate to chemoresistance [42, 45], once again implicating drug resistance in metastatic cancers. Eventually, once these cells have metastasised and travelled to alternate locations in the body, they will undergo the reverse process – known as mesenchymal to epithelial transition (MET) – which will enable the cancer to grow and proliferate in its new locale [43].

1.6 Cell Adhesion

Adhesion of cells to the ECM by cell membrane proteins, such as integrins, can elicit intracellular signalling cascades. In this way, cellular adhesion to the ECM can be involved in drug resistance through altered signalling pathways being initiated by the adhesion events [46]. Metastatic and drug-resistant cancers can be better at navigating the ECM. In order to facilitate movement through the ECM, cells must degrade some components in order to clear a pathway to travel through.

Cell adhesion is mediated by a multitude of proteins and structures. One of the primary components of the ECM is fibronectin (FN). FN provides not only structural elements to the ECM, but it also gives anchoring points for cells to the ECM [47]. Additionally, this cellular anchoring to FN is involved in signalling activities [46]. This signalling occurs through a variety of pathways, primarily through integrins. Integrins bind to FN in a ligand-receptor manner with the arginine-glycine-aspartic acid (RGD) sequence on fibronectin being the ligand and the integrin the receptor. The RGD motif has been shown to play a role in cancer metastasis, particularly the EMT and MET changes that cells undergo [48, 49]. Cellular adhesion can mediate drug resistance in cancer [50, 51].

Matrix metalloproteinases (MMPs) are proteins that cells use to facilitate ECM degradation. In some cases, drug-resistant and metastatic cancers have elevated MMPs [52], and the inhibition of these MMPs could potentially improve treatment of drug-resistant cancers, such as in ovarian cancer [53].

1.7 Carboxylesterase

Carboxylesterase enzymes (CES) are ubiquitously distributed throughout the body. There are two main forms; carboxylesterase 1 (CES1), found primarily within the liver, and carboxylesterase 2 (CES2), which is located in the intestinal cells [54]. CES2 located on the external cell membranes can catalyse extracellular reactions and CES2 present within the cells contributes to intracellular metabolism.

CES metabolises irinotecan and converts it into the active metabolite SN-38. The primary site of activation is in the liver – where CES1 is abundant – because irinotecan is administered as an intravenous infusion. Irinotecan is not in direct contact with the lumen of the intestines, diminishing the role of CES2 in the initial metabolism. Irinotecan that passes through the liver and is not converted can potentially be converted by intestinal cells as they are supplied with blood. CES2 exhibits a higher rate of hydrolysis than CES1 [55], which is likely related to the broader substrate specificity of CES1 [56].

CES can be inhibited by loperamide, a drug used to stop symptomatic diarrhea that occurs as a result of treatment with irinotecan. Although inhibition of the enzyme responsible for the metabolism of irinotecan into SN-38 seems counter-intuitive as a clinical strategy, there is not a significant decrease in the therapeutic effectiveness of irinotecan when treating diarrhea symptoms with loperamide [57]. Additionally, loperamide likely has a greater effect on CES2 due to low bioavailability and its primary action on enzymes within the gut. Loperamide is, however, metabolised by CYP enzymes in the liver [58].

1.8 Glutathione S-Transferase

Glutathione S-transferase (GST) is an enzyme that conjugates reduced glutathione (GSH) to xenobiotics to facilitate their removal; these substances are then secreted into bile for excretion. GST is also involved in inflammatory responses, which is important considering the inflammatory nature of cancer as a disease.

There are several isoforms of GST. The isoform that is largely responsible for drug inactivation and removal in humans is GST pi (GSTP). In particular, GSTP1-1 removes drugs from the body and inactivates compounds. GSTP has elevated expression in proliferating cells [59]. In addition to this, GSTP is implicated in several cancers and drug-resistance mechanisms [60]. GST can be upregulated when cells are exposed to anticancer drugs, including irinotecan. In a study from 2002, partial sensitivity to irinotecan was returned to cells following treatment with a GSTP inhibitor [60].

GST is also relevant to MAPK pathways, which are important in signalling cascades. Cytosolic GST plays a role of inhibition in MAPK pathways, and acts on cell signalling molecules for survival and inhibition of cell death. This could mean that rather than detoxification of cells, GST may be involved in alteration of survival and apoptotic signalling [61]. Of note, GSTP1 binds to JNK; this binding inhibits the downstream apoptotic signalling elicited by JNK1 [62]. When it is unbound to GSTP1, JNK normally signals the Bcl-2-family protein Bax, which has further downstream signals that result in the promotion of apoptosis.

GSTP exists in both a monomeric and a dimeric state. When in the dimeric configuration, GSTP functions primarily to clear xenobiotics from the cells [62]. In the monomeric state, GSTP has been shown to form protein complexes with JNK, in particular with JNK1 [62].

1.9 Rationale for the Project

Drug resistance in CRC heavily contributes towards the poor outcomes in patients. Considering the lethality of metastatic and drug-resistant CRC, it is important to gain a greater understanding of how metastatic and drug-resistant CRC differ from drug-sensitive and localised CRC. The aim of this project was to study these differences and elucidate some of the cellular behavioural and enzymatic changes that contribute to these alterations in patient outcomes. GST was chosen as an enzyme of importance to study due to its implication in drug resistance. CES enzymes were selected for their involvement in both drug resistance and irinotecan metabolism. Through this research greater insight into how drug-resistant CRC evades death may be gained.

1.10 Hypothesis and Objectives

Hypothesis

Drug resistance in colorectal cancer confers increased adhesion, and is promoted by the presence and activity of the metabolic enzymes carboxylesterase and glutathione S-transferase.

The objectives of my project were to identify and quantify changes in:

1. Adhesion of HT29 and SN-38-resistant HT29-S colon carcinoma cells on a fibronectin substratum and a HepG2 hepatocellular carcinoma monolayer
2. 5-chloromethylfluorescein diacetate conversion between SN-38-sensitive and SN-38-resistant colon carcinoma cells
3. Carboxylesterase activity in SN-38-sensitive and SN-38-resistant colon carcinoma cells
4. Glutathione S-transferase activity in SN-38-sensitive and SN-38-resistant colon carcinoma cells

Chapter 2. Methods

2.1 Cell Culture

The six cell lines listed in Table 1 were cultured for this study. The cell lines HT29, HCT116, Caco-2, and HepG2 were obtained from American Type Culture Collection (Manassas, VA, United States). The HT29-S and HCT116-S cell lines were established by Dr. Murray Cutler through successive treatment of HT29 and HCT116 cells with low levels of SN-38 (Sigma Aldrich) increased to a concentration of 30 nM SN-38, and were resistant to cytotoxicity by SN-38. HT29-S and HCT116-S were cultured with 30 nM of SN-38 to maintain the drug-resistant phenotype. All cell lines were cultured using Dulbecco's modified Eagle's medium (DMEM; HyCLone Laboratories Inc.) with additional additives to the media such as new-born calf serum (NCS; ThermoFisher Scientific) and fetal bovine serum (FBS; VWR International).

Table 1 Cell lines and cell culture components

Cell Line	Media	Additions
HT29	5% FBS,10% NCS	
HT29-S	5% FBS, 10% NCS	30 nM SN-38
HCT116	10% NCS	
HCT116-S	10% NCS	30 nM SN-38
Caco-2	5% FBS	
HepG2	5% FBS	

2.2 Staining Cells with 5-chloromethylfluorescein diacetate (CMFDA)

The six cell lines were cultured in T25 flasks (Nunc™) and grown to 80-90% confluence. The media were aspirated off and cells released using 1 mL of 0.25% trypsin-ethylenediaminetetraacetic acid (EDTA; Gibco™) followed by incubation at 37 °C for 10-15 min. To inactivate the trypsin-EDTA, the cells were suspended in 5 mL of DMEM 10% FBS for the HT29-S, HepG2, and Caco-2 cells, and 10% NCS for the HT29, HCT116, and HCT116-S cells. The cells were centrifuged using an Allegra X-22R Centrifuge (Beckman Coulter) at 400 x g for 3 min at 4 °C and the supernatant removed. The cells were suspended in serum-free DMEM to a concentration of 50 000 cells/mL; 5 µL/mL of 5-chloromethylfluorescein diacetate (CMFDA) was added and the cell suspensions incubated at 37 °C for 30 min to stain. Cells were centrifuged again at 400 x g at 4 °C for 3 min. The supernatant was removed and the cells suspended in 10% FBS, then incubated for a further 30 min at 37 °C to wash away excess CMFDA. Cells were centrifuged for a final time at 400 x g for 3 min at 4 °C, then suspended in DMEM with or without FBS or NCS according to the conditions necessary for each experiment and cell line.

2.3 Cell Adhesion Assays

2.3.1 Cell adhesion assays on glass coverslips

Glass coverslips that were 22 mm in diameter (ThermoFisher Scientific) were placed in 24-well plates and coated with 300 µL of 100 µg/mL Poly-L-lysine (PLL; Sigma Aldrich) in MilliQ H_2O and incubated at 37 °C for 10 min. Excess PLL solution was removed and the coverslips allowed to dry at room temperature. Cell suspensions were stained using CMFDA. 50 000 cells, stained with CMFDA, in 500 µL were added onto the coverslips and incubated at 37 °C for 2.5 h for adhesion. Following the adhesion period, coverslips were gently washed with phosphate buffered saline (PBS) to remove any cells that were unadhered. The coverslips were mounted on glass slides using a drop Fluoroshield aqueous gel mountant containing 1 µg/mL 2-(4-amidinophenyl)-1H-indole-6-carboxamidine (DAPI; Abcam). Slides were protected from the light and dried overnight at room temperature. Fluorescence was detected using a Leica DM2000 light microscope. Images were taken using a QImaging Micropublisher 5.0 RTV camera and QCapture Pro software.

2.3.2 Cell adhesion on a fibronectin substratum

4-well plates were coated with 500 µL of 5 µg/mL bovine plasma fibronectin (Sigma Aldrich) in MilliQ H_2O overnight at 4 °C. The remaining fibronectin solution was removed the following day and 500 µL of 2% bovine serum albumin (BSA; Sigma Aldrich) in serum-free DMEM was applied for 10 min at room temperature as a blocking solution. HT29 and HT29-S cells were released from their T25 flasks using 1 mL of TrypLE Express enzyme (Life Technologies) and suspended in 4 mL of DMEM 10% FBS to inactivate the TrypLE enzyme. Cells were collected and centrifuged using an Allegra X-22R Centrifuge (Beckman Coulter) at 400 x g for 3 min at 4 °C. The supernatant was discarded and the cells suspended in 5 mL of cold PBS to wash away remaining serum. The cells were centrifuged at 400 x g for 3 min at 4 °C, and the supernatant discarded; the cells were suspended in 5 mL of serum-free DMEM and counted using a Multisizer 4 Coulter Counter (Beckman Coulter) to determine the concentration of this suspension. The cells were diluted to a concentration of 100 000 cells/mL and stained with CMFDA. 500 µL of the cell suspension was added to each well of the fibronectin coated 4-well plates and the plates incubated at 37 °C for 2.5 h to allow for adhesion. Following the adhesion period, coverslips were gently washed with PBS to remove any unadhered cells. Fluorescence was detected using a Leica DM2000 light microscope. Images were taken using a QImaging Micropublisher 5.0 RTV camera.

2.3.3 Cell adhesion on a HepG2 hepatocellular carcinoma monolayer

4-well plates were seeded with 500 µL of a HepG2 cell suspension, and incubated at 37 °C, 5% CO_2 until the HepG2 cells were approximately 90% confluent. After the HepG2 monolayer was grown, the medium was removed and the wells washed using PBS. 300 µL of 3.7% paraformaldehyde (PFA; Sigma Aldrich) was used to fix the HepG2 cells in a control well. HT29 and HT29-S cells were released from their T25 flasks using 1 mL of TrypLE Express enzyme (Life Technologies) and suspended in 4 mL of DMEM 10% FBS to inactivate the TrypLE enzyme. Cells were collected and centrifuged using an Allegra X-22R Centrifuge (Beckman Coulter) at 400 x g for 3 min at 4 °C. The supernatant was discarded and the cells suspended in 5 mL of cold PBS to wash away remaining serum; the cells were centrifuged again at 400 x g for 3 min at 4 °C. The supernatant was discarded and the cells were suspended in 5 mL of serum-free DMEM and counted using a Multisizer 4 Coulter Counter (Beckman Coulter) to determine the concentration of the suspension. The cells were stained with CMFDA. 50 000 cells, stained with CMFDA, in 500 µL were added to each well of the 4-well plates and the plates were incubated at 37 °C for 2.5 h to allow for adhesion. Following the adhesion period, the wells were gently washed with PBS to remove any unadhered cells. Fluorescence was detected using a Leica DM2000 light microscope and images were captured using a QImaging Micropublisher 5.0 RTV camera.

2.4 5-chloromethylfluorescein diacetate (CMFDA) Conversion Experiment

The six cell lines were cultured in T75 flasks (Nunc™) and grown to 80-90% confluence. The media were aspirated off and cells released using 3 mL of 0.25% trypsin-EDTA (Gibco™) followed by incubation at 37 °C for 10-15 min. To inactivate the trypsin-EDTA, the cells were suspended in 5 mL of DMEM 10% FBS for the HT29-S, HepG2, and Caco-2 cells, and 10% NCS for the HT29, HCT116, and HCT116-S cells. The cells were counted using a Multisizer 4 Coulter Counter (Beckman Coulter) and separated at 1 x 10^6 cells per tube into 1.5 mL Eppendorf tubes. The cells were stained using CMFDA with an adjusted protocol involving extended incubation periods – a 1 h stain period followed by a 30 min wash out period. Unstained cells were used as controls. The cells were centrifuged using a 5424R microcentrifuge (Eppendorf) at 400 x g for 10 min at 4 °C. Supernatant was removed using gentle aspiration. The lysis buffer (A.1.3 Lysis Buffer) was added to the cells and the tubes were agitated intermittently for approximately 30 min until the cells were lysed and well homogenised. The lysate was centrifuged at 14 000 x g for 5 min at 4 °C using a 5424R microcentrifuge (Eppendorf). 200 µL of the supernatant was transferred into a 96-well plate. Fluorescence levels were measured using a spectrofluorometer (SpectraMax M5) and excitation and emission wavelengths of 492 nm and 517 nm respectively.

2.5 Carboxylesterase Activity Assays

2.5.1 4-methylumbelliferyl acetate (4-MUBA) conversion

HT29, HT29-S, HCT116, HCT116-S, HepG2, and Caco-2 cells were cultured in 24-well plates using eight wells per cell line, and grown to 80-90% confluence. The media were removed and cells were released from four wells per cell line using 200 µL of 0.25% trypsin-EDTA and incubated at 37 °C, 5% CO_2 for 10-15 min. The released cells were counted using the Multisizer 4 Coulter Counter (Beckman Coulter). 100 µL of lysis buffer was added to the remaining wells and the plate was placed at 4 °C for 10 min. The plates were agitated and the lysates from each well collected and transferred into individual 1.5 mL Eppendorf tubes, using 1 tube per well. The lysates were separated using a 5424R microcentrifuge (Eppendorf) at 14 000 x g for 10 min at 4 °C. A 96-well plate was prepared and 120 µL of a 0.083 mM 4-methyumbelliferyl acetate (4-MUBA; Alfa Aesar) substrate solution in KPBS Ca^{2+} Mg^{2+} (Appendix A.1.4 Phosphate Buffer with Ca2+ Mg2+) was added to the respective wells – four wells per cell line plus an additional four wells for blanks. 80 µL of supernatant from the centrifuged tubes was added to the 4-MUBA filled wells, and the solutions gently mixed. 80 µL of the lysis buffer was added to the blank wells. Fluorescence readings were measured at 10 min intervals over a 3 h period (Figure 5) at room temperature using a SpectraMax spectrofluorometer (Molecular Devices) set to 350 nm emission and 450 nm excitation parameters. The results were normalised by subtracting the blank values, then adjusting the resulting values to cell counts obtained from the four wells of each cell line. A fixed assay time of 2.5 h was chosen based on the results found in Figure 5.

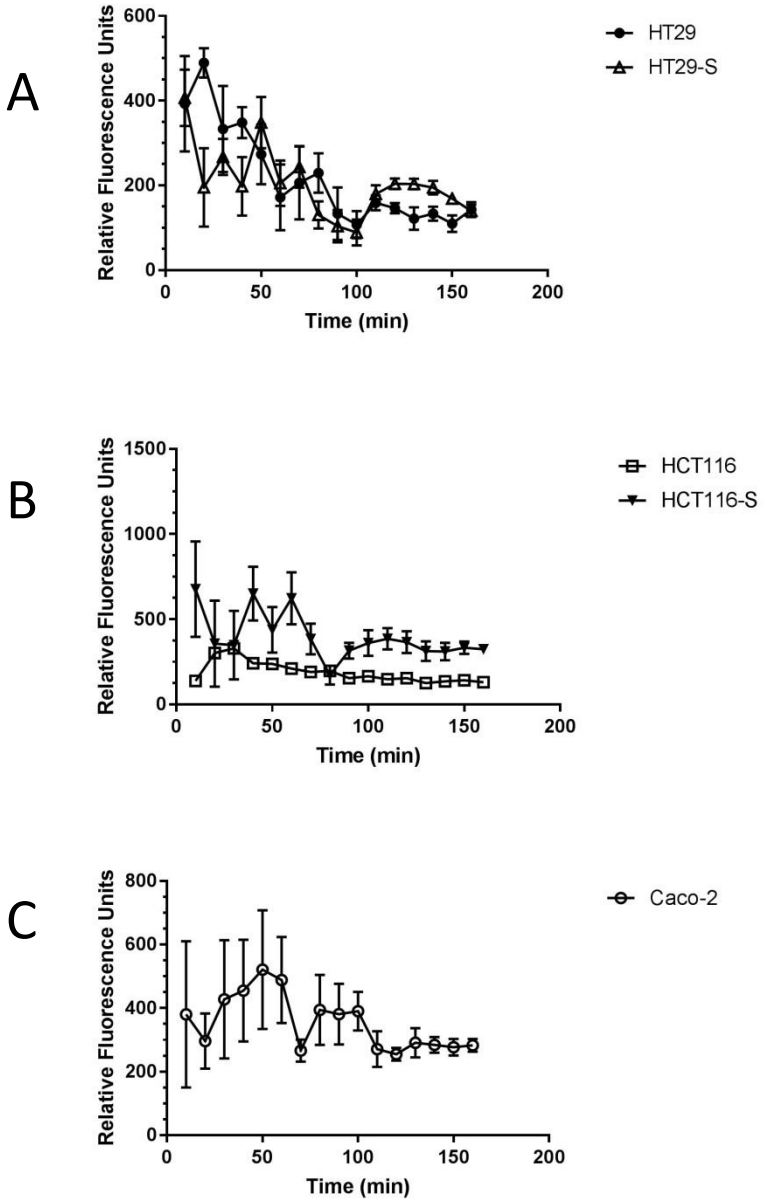

Figure 5 Time course of carboxylesterase activity in colon cancer cells using 4-methylumbelliferyl acetate

HT29 and HT29-S (A), HCT116 and HCT116-S (B), and Caco-2 (C) cells were grown to 90% confluence. The cells were counted and lysed. 80 µL of lysate was placed in a 96-well plate, and 120 µL of 0.083 mM 4-methyumbelliferyl acetate substrate added to reach a final concentration of 0.05 mM. The data are mean relative fluorescence units ± SEM of three technical replicates plotted over a 3 h time course with readings taken every 10 min. The blank control values were subtracted and resulting values normalised to the cell counts for each cell line.

Solutions used in the 4-MUBA assays showed some fluorescence (Figure 6), but this was determined to be of little interference in the 4-MUBA assays themselves when using blank control wells of the solutions. There were higher fluorescence readings from the black plates for most of the solutions used except KPBS Ca^{2+} Mg^{2+}. These results indicated that the clear plates are less likely to influence the fluorescence readings and were selected for further use.

A

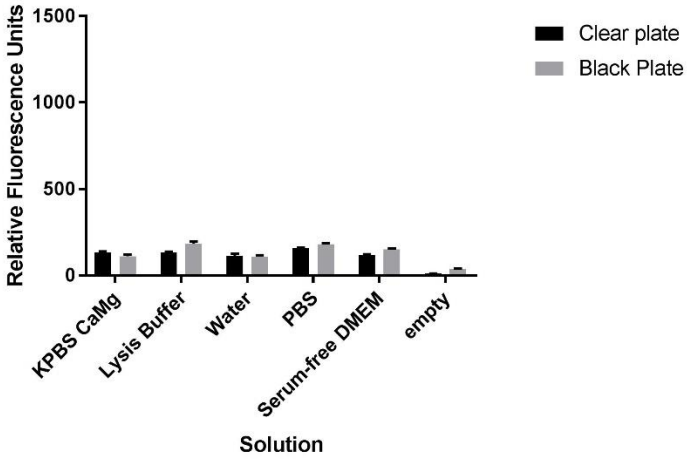

B

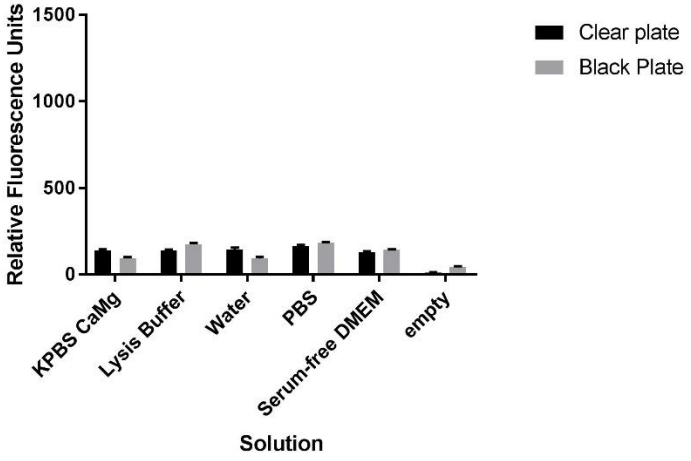

Figure 6 Fluorescence of clear and black 96-well plates and solutions used in 4-methylumbelliferyl acetate experiments

Black and clear plates were selected to compare potential fluorescent interference between wells. The solutions used in the 4-methylumbelliferyl acetate assays were assessed for their potential fluorescence. Panels A and B are experimental replicates. The data are means are of three technical replicates ± SEM.

2.5.2 p-nitrophenyl acetate (pNP) conversion

24-well plates were seeded with HT29, HT29-S, HCT116, HCT116-S, HepG2, and Caco-2 using eight wells per cell line, 500 µL per well. The cells were grown to 80-90% confluent. The media were aspirated from the wells, and the cells released from four wells per cell line using 200 µL of 0.25% trypsin-EDTA and incubation at 37 °C, 10% CO_2 for 10-15 min. The cells were counted using the Multisizer 4 Coulter Counter (Beckman Coulter) and a Modified Neubauer hemocytometer. A solution of 2 mM p-nitrophenyl acetate (pNP) in 50 mM trisHCL buffer (pH 7.0) was prepared. The 24-well plates were washed twice using 500 µL of cold PBS per well. The PBS was gently aspirated and 250 µL of the pNP solution was added to each of the four remaining wells. The plates were incubated at 37 °C, 10% CO_2 for 2 h. A plate with 2 mM pNP solution was kept in the same conditions as the plates containing cells and served as a blank. 50 µL of supernatant was removed and transferred to a 96-well plate at 20 min, 40 min, and 120 min intervals over the incubation period. Absorbance values were measured at a 405 nm wavelength using the SpectraMax spectrophotometer (Molecular Devices). These values were normalised to the cell counts acquired for each cell line following subtraction of the blank values (Figure 7). After the initial optimisation experiments, HepG2 cells were deemed unnecessary for the further experiments.

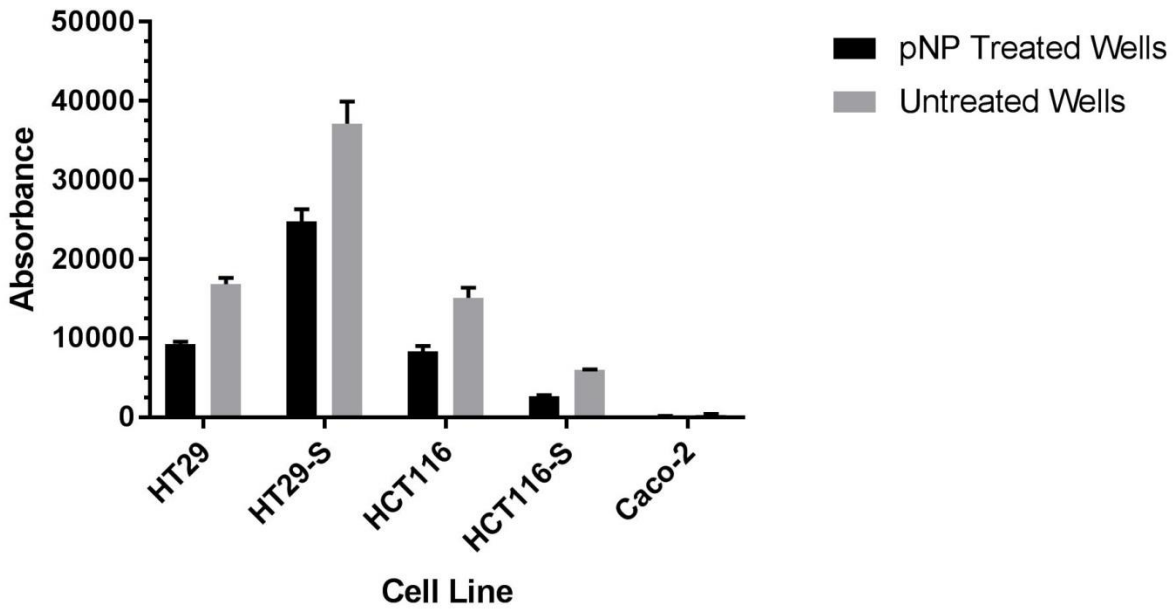

Figure 7 Cytotoxicity of 2.0 mM p-nitrophenyl acetate in different colon cancer cells
50 000 cells were added to 24-well plates and grown to 90% confluence. Half of the wells were treated with the 2.0 mM p-nitrophenyl (pNP) acetate solution and the other half untreated. The pNP treated wells display high levels of cytotoxicity to cells after an exposure of 2 h. Data presented are means ± SEM of three technical replicates normalised to cell counts. Blank values were subtracted from absorbances and the resulting values adjusted to cell counts for each cell line.

Following the initial pNP assay, six concentrations of pNP were used. HT29, HT29-S, HCT116, HCT116-S, and Caco-2 cells were cultured in 24-well plates, one plate per cell line, and grown to 80-90% confluence. The media were aspirated from the wells, and cells were released from six wells of each cell line by using 200 µL of 0.25% trypsin-EDTA and incubation at 37 °C, 10% CO_2 for 10-15 min. The cells were counted using a Multisizer 4 Coulter Counter (Beckman Coulter) and a Modified Neubauer hemocytometer. The media were aspirated from the remaining wells and the cells washed twice with 500 µL of cold PBS. 250 µL of pNP in 50 mM trisHCl buffer (pH 7.0) was added to the wells. The plates were incubated for 2 h at 37 °C, 10% CO_2. A 24-well plate with wells filled with each of the six concentrations of pNP was incubated in the same conditions to serve as the blanks. 50 µL of supernatant was transferred from each well to a 96-well plate at 20 min, 40 min, and 120 min time intervals during the incubation period (Figure 8). Absorbance values were measured at a 405 nm wavelength using the SpectraMax spectrophotometer (Molecular Devices). The acquired absorbance values were normalised by subtracting the blanks and adjusting the resulting values to the cell counts for each cell line.

Based on the data acquired in Figure 8, it was determined that 40 min was the optimal time interval to use. This was supported by the decrease in activity at 120 min, which is likely explained by the cytotoxic effects of the substrate, as identified in Figure 7.

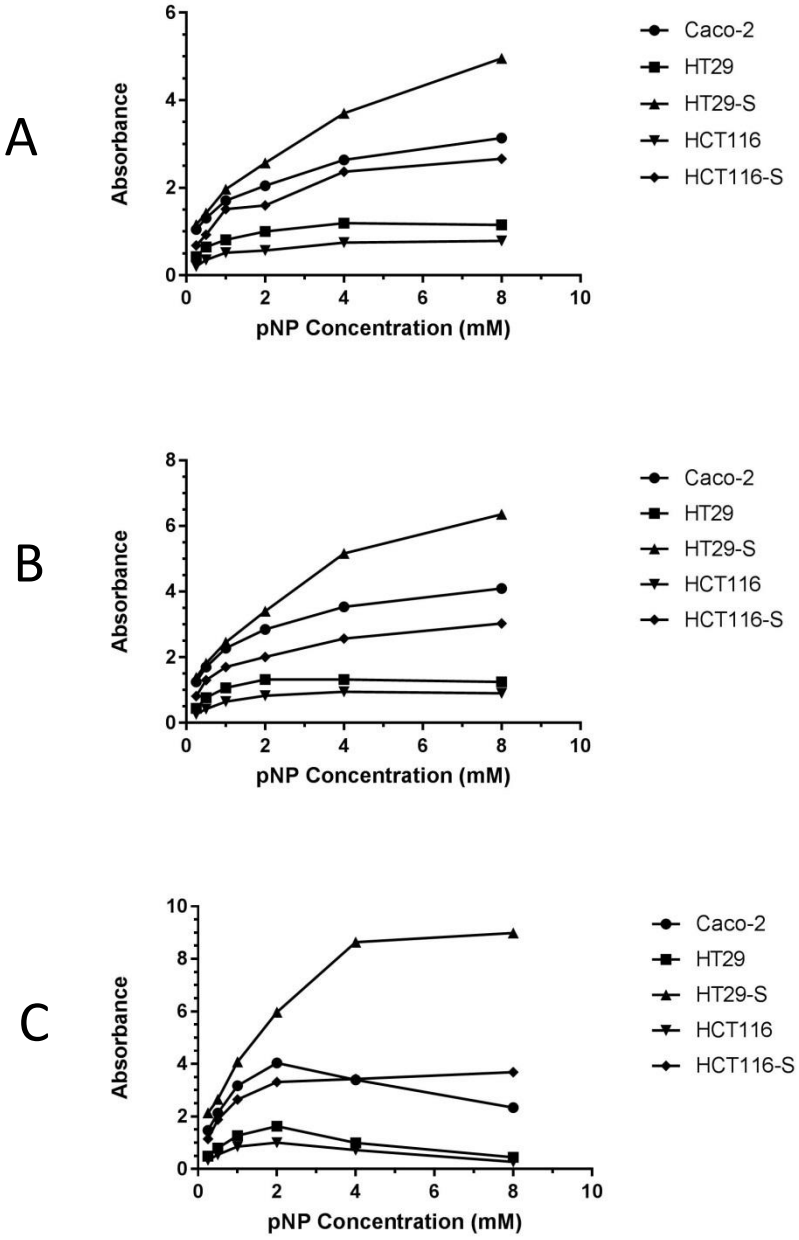

Figure 8 Conversion of p-nitrophenyl acetate in different colon cancer cells

Cells were grown to approximately 90% confluence in 24-well plates. Six concentrations of p-nitrophenyl acetate were added and the cells incubated at 37 °C, 5% CO_2. Supernatant was removed at 20 min (A), 40 min (B), and 120 min (C) time intervals and absorbance measured at 405 nm. Blank values were subtracted from absorbances and the resulting values adjusted to cell counts for each cell line.

2.6 Glutathione S-Transferase Activity Assay

HT29, HT29-S, HCT116, HCT116-S, and Caco-2 cells were cultured in 24-well plates using twelve wells per cell line, and grown to 80-90% confluence. The media were aspirated from the wells and cells released using 200 µL of 0.25% trypsin-EDTA and incubation at 37 °C, 10% CO_2 for 10-15 min. The cells were counted from six wells per cell line using a Multisizer 4 Coulter Counter (Beckman Coulter) and a Modified Neubauer hemocytometer. The contents of the remaining six wells were suspended in separate 1.5 mL Eppendorf tubes, one tube per well. The cells were centrifuged at 500 x g for 10 min at 4 °C using a 5424R microcentrifuge (Eppendorf). The supernatant was gently removed and the pelleted cells suspended in 80 µL of lysis buffer and agitated intermittently for 20-30 min until homogenised. The contents of the tubes were centrifuged at 14 000 x g for 5 min at 4 °C using a 5424R microcentrifuge (Eppendorf). 20 µL of supernatant was transferred to a 96-well plate prepared using 1 mM 1-chloro-2,4-dinitrobenzene (CDNB) and 2 mM reduced glutathione (GSH) as substrates, see Table 2 for the preparation of the 96-well plate. The reaction time was 10 min at room temperature with absorbance values measured at 2 min intervals (Figure 9), a fixed endpoint of 10 min was used for further GST activity assays. Absorbance values were measured at 340 nm using the SpectraMax spectrophotometer (Molecular Devices) and normalised by subtracting the blanks and adjusting the resulting values by the cell counts for each cell line.

Table 2 Solution volumes for glutathione S-transferase activity experiments using 1 mM 1-chloro-2,4-dinitrobenzene (CDNB) and 2 mM reduced glutathione (GSH)

Label	Supernatant	CDNB + GSH Substrate	Lysis buffer	Number of wells
HT29	20 µL	180 µL	0 µL	6
HT29-S	20 µL	180 µL	0 µL	6
HCT116	20 µL	180 µL	0 µL	6
HCT116-S	20 µL	180 µL	0 µL	6
Caco-2	20 µL	180 µL	0 µL	6
Substrate Blank	0 µL	180 µL	20 µL	6
Blank	0 µL	0 µL	200 µL	6

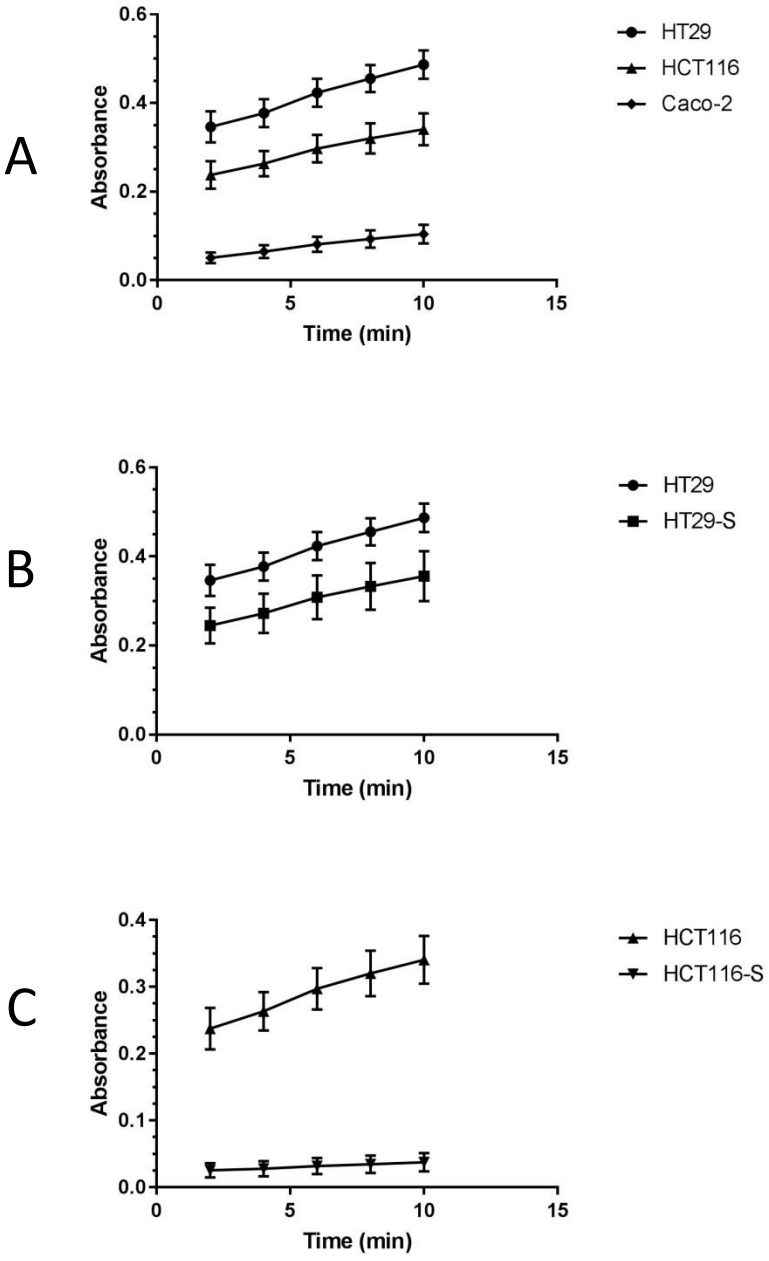

Figure 9 Glutathione S-transferase activity in different colon cancer cells

Time course evaluation of glutathione S-transferase activity using cell lysates from HT29 (A,B), HT29-S (B), HCT116 (A,C), HCT116-S (C), and Caco-2 (A) cell lines. 1 mM of 1-chloro-2,4-dinitobenzene and 2 mM reduced glutathione were used as substrates. Absorbance readings were taken at a 340 nm wavelength every 2 min for 10 min. Data are means presented ± SEM of three technical replicates normalised by subtracting blanks and adjusting the resulting values to the cell counts of each cell line.

HT29, HT29-S, HCT116, HCT116-S, HepG2, and Caco-2 cells were cultured in 24-well plates with twelve wells per cell line, and grown to 80-90% confluence. The media were aspirated from the wells and the cells released using 200 µL of 0.25% trypsin-EDTA and incubation at 37 °C, 10% CO_2 for 10-15 min. The cells from six wells per cell line were counted using a Multisizer 4 Coulter Counter (Beckman Coulter) and a Modified Neubauer hemocytometer. The contents of the remaining six wells were suspended in separate 1.5 mL Eppendorf tubes, using one tube per well. The cells were centrifuged at 500 x g for 10 min at 4 °C using a 5424R microcentrifuge (Eppendorf). The supernatant was gently removed and the pelleted cells suspended in 80 µL of lysis buffer and agitated intermittently for 20-30 min until homogenised. The contents of the tubes were separated using a 5424R microcentrifuge (Eppendorf) at 14 000 x g for 5 min at 4 °C. 20 µL of the supernatant was transferred to a 96-well plate prepared using CDNB and GSH as substrates in a 1:2 ratio, see Table 3 for the 96-well plate set-up volumes. The reaction took place over the course of 10 min at room temperature. Absorbance values were measured at 340 nm using the SpectraMax spectrophotometer (Molecular Devices) and absorbance values were normalised by subtracting the blanks and adjusting the resulting values to the cell counts for each cell line.

Table 3 Solution volumes for glutathione S-transferase activity experiments using six concentrations of 1-chloro-2,4-dinitrobenzene (CDNB) and reduced glutathione (GSH)

Label	Supernatant	CDNB + GSH Substrate	Lysis buffer	Number of wells
HT29	20 µL	180 µL	0 µL	3 per concentration
HT29-S	20 µL	180 µL	0 µL	3 per concentration
HCT116	20 µL	180 µL	0 µL	3 per concentration
HCT116-S	20 µL	180 µL	0 µL	3 per concentration
HepG2	20 µL	180 µL	0 µL	3 per concentration
Caco-2	20 µL	180 µL	0 µL	3 per concentration
Substrate Blank	0 µL	180 µL	20 µL	3 per concentration
Blank	0 µL	0 µL	200 µL	3

2.7 Statistical Analysis

Experiments were performed with technical triplicate, and repeated as several independent experiments for biological replicates. For quantitative measurements, results were reported as the mean ± standard error of the mean (SEM). For non-quantitative experiments, the data selected and presented were representative of all the results. One-way and two-way ANOVAs were used along with either Bonferroni or Dunnett's multiple comparisons tests as appropriate. GraphPad Prism® software was used to perform data analysis.

2.8 Generation of Figures

Figure 1, Figure 3, Figure 4, Figure 17, and Figure 18 were adapted from Servier Medical Art by Servier, licensed under CC 3.0. https://smart.servier.com/image-set-download/ (accessed September, 2018).

Chapter 3. Results

3.1 Cell Adhesion

3.1.1 Overview

I wished to test the adhesion of the HT29 and SN-38-resistant HT29-S colon cancer cells, and to determine if the drug-resistant cells had a higher capacity for adhesion than the drug-sensitive cells. The ability of these cells to adhere to fibronectin as a main component of the ECM was first assessed; following that, I wished to observe the interaction of the cells with a more complex ECM. HepG2 hepatocellular carcinoma cells were used to provide a more complex ECM and functioned as a model liver environment, simulating the primary metastatic site of CRC.

3.1.2 Adhesion of HT29 and SN-38-resistant HT29-S cells to fibronectin

To assess the adhesion of drug-sensitive and drug-resistant cells to fibronectin, HT29 and HT29-S cells were stained with CMFDA and added to fibronectin-coated wells. After 2 h of incubation at 37 °C, the drug-sensitive cells had lower levels of adhesion compared to the drug-resistant cells. This can be seen in Figure 10. The HT29-S cells were also more heavily clustered, and had irregular shapes and sizes compared to the HT29 drug-sensitive cells.

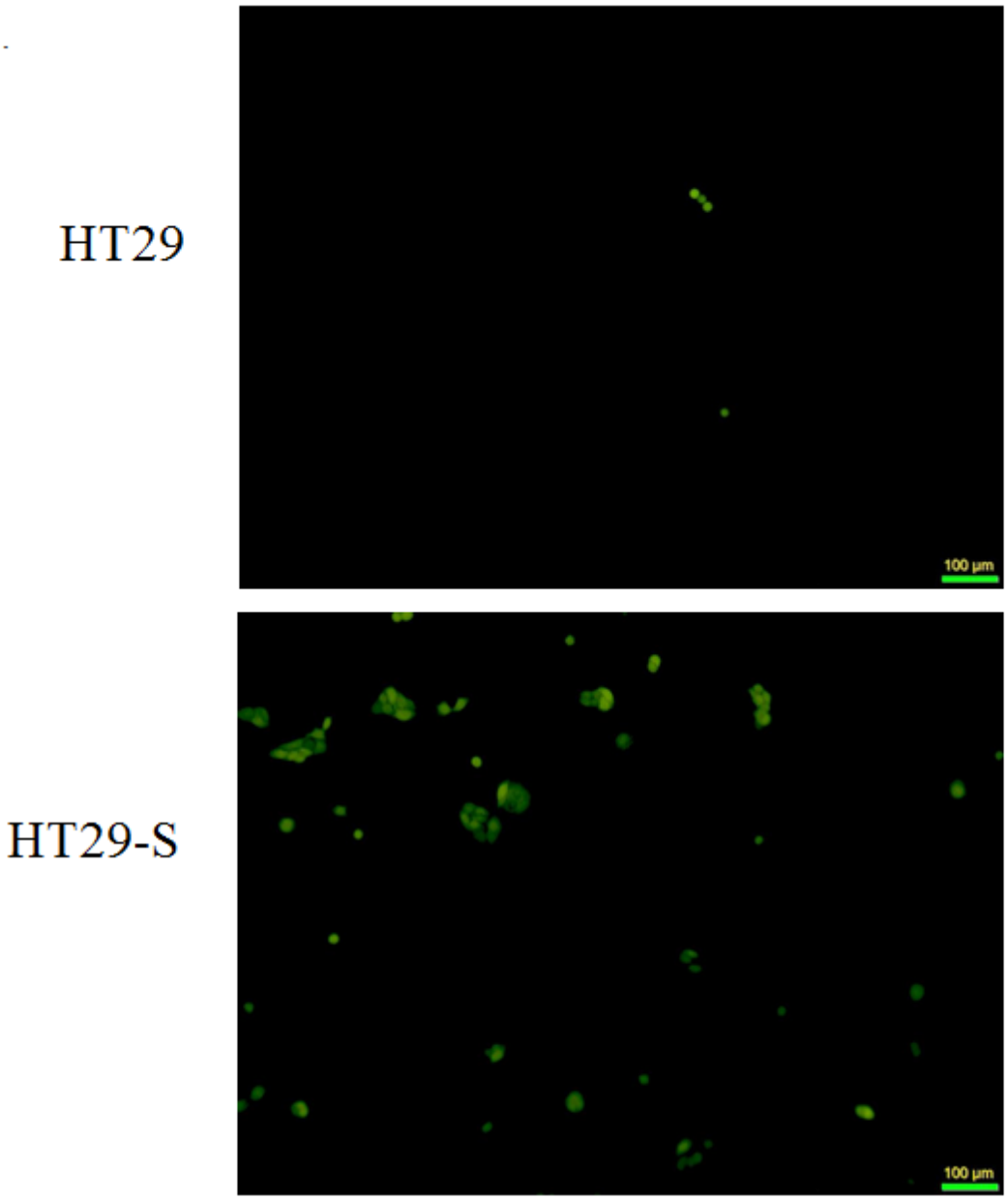

Figure 10 Increased adhesion of SN-38-resistant HT29-S colon cancer cells to fibronectin
HT29 (top) and HT29-S (bottom) adhered to wells coated with 500 µL of 5 µg/mL solubilised fibronectin. 50 000 cells, stained with CMFDA, in 500 µL of serum-free DMEM were added to the fibronectin coated wells. The cells were allowed to adhere for 2.5 h at 37°C, 5% CO_2. The plates were gently rinsed in ice-cold PBS, and images taken using QCapture Pro.

3.1.3 Adhesion of HT29 and SN-38-resistant HT29-S cells to HepG2 hepatocellular carcinoma cells

Following these observations using FN, I wanted to assess the adhesion behaviours in a more complex ECM environment. To accomplish this, monolayers of HepG2 hepatocellular carcinoma cells were grown in the wells. A bright field image of the monolayer can be seen in Figure 11 along with the fluorescent image of adhered HT29 cells in the same field of view. CMFDA-stained HT29 and HT29-S cells were added to the wells and incubated at 37 °C for 2.5 h. Adhesion of the HT29 and HT29-S cells was observed using fluorescent microscopy. The numbers of cells adhered were greater for both HT29 and HT29-S when compared to adhesion to the FN substratum. This increase in adhesion is understandable given the multitude of other components the cells can adhere to within a fully established ECM. There was a substantial increase in the adhesion of HT29-S cells compared to the HT29 cells (Figure 12). Irregularity of size and shape, and cell clustering was observed again in the HT29-S cells as seen in Figure 12.

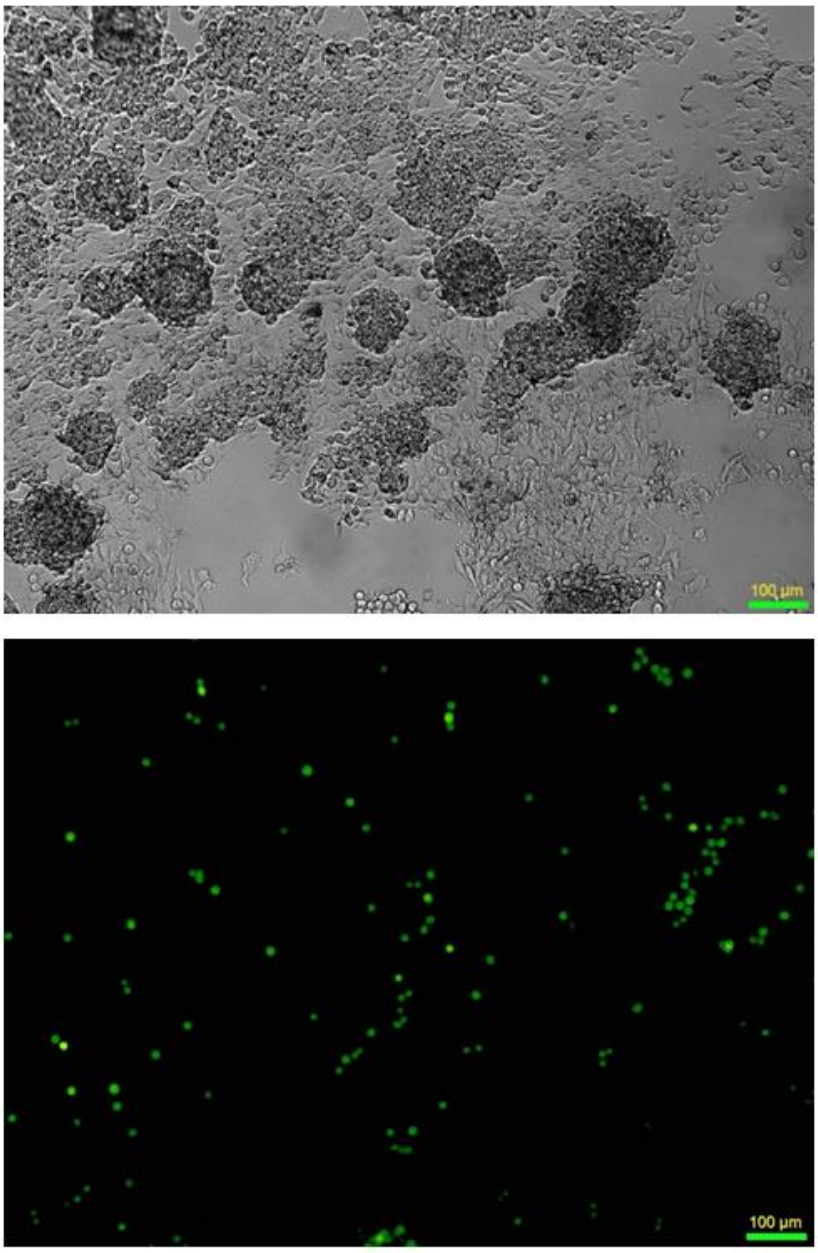

Figure 11 HT29 colon cancer cells adhered to a HepG2 hepatocellular carcinoma monolayer

Bright field (top) and fluorescent (bottom) images of HT29 cells bound to a HepG2 hepatocellular carcinoma monolayer. 50 000 HT29 cells, stained with CMFDA, in 500 µL of serum-free DMEM were added to HepG2 monolayer coated wells in a 4-well plate at 37 °C, 5% CO_2 for 2.5 h. The plates were gently rinsed with ice-cold PBS and images taken using QCapture Pro.

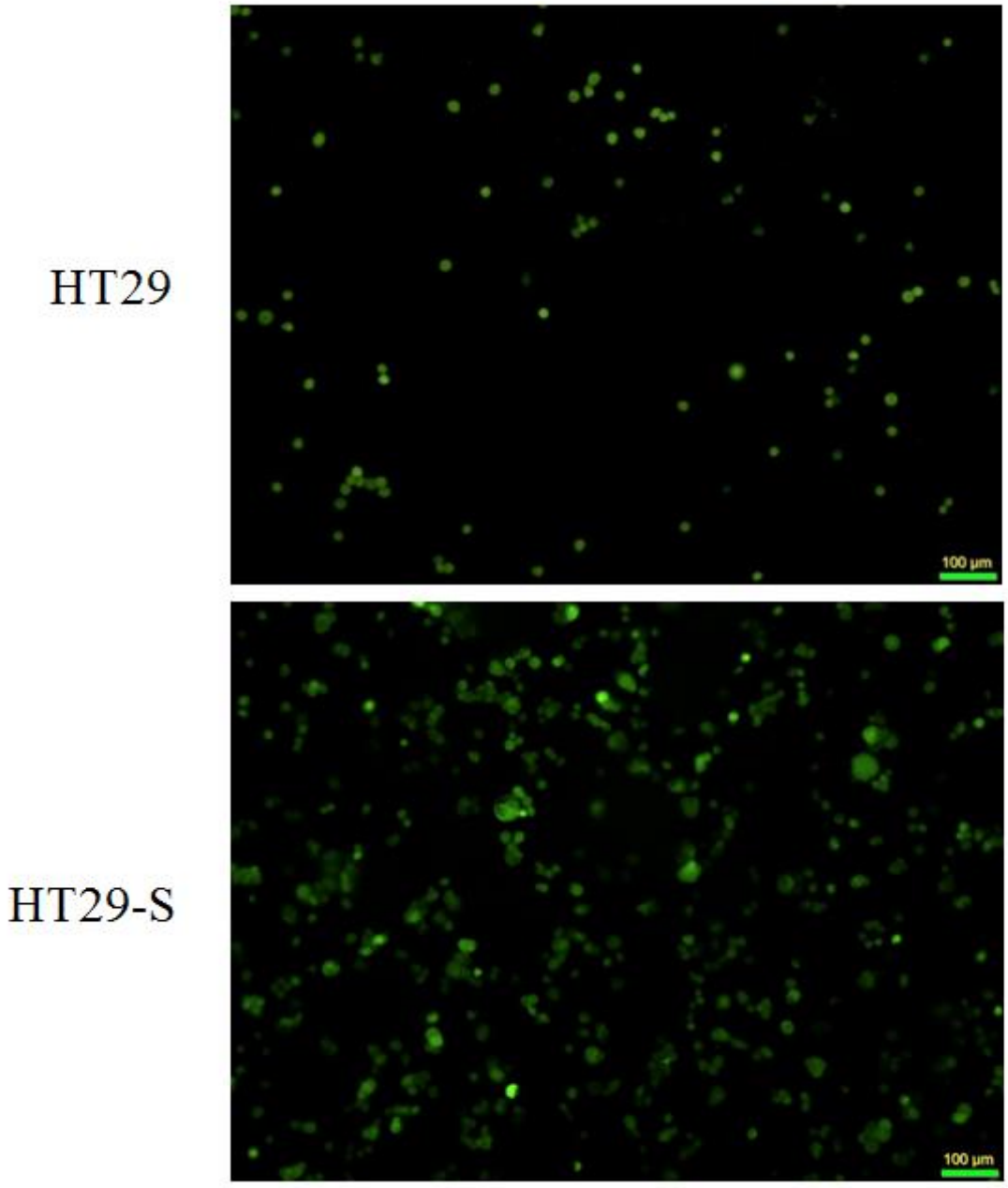

Figure 12 Increased adhesion of SN-38-resistant HT29-S colon cancer cells on a HepG2 hepatocellular carcinoma monolayer

HT29 (top) and HT29-S (bottom) images of HT29 cells bound to a HepG2 hepatocellular carcinoma monolayer. 50 000 cells, stained with CMFDA, in 500 µL were added to the respective wells coated with a HepG2 monolayer, and allowed to adhere for 2.5 h at 37 °C, 5% CO_2. The plates were gently rinsed using ice-cold PBS and images taken using QCapture Pro.

3.2 5-chloromethylfluorescein diacetate (CMFDA) Conversion in Colon Cancer Cells

During the cell adhesion experiments, I noticed on multiple occasions that the HT29-S SN-38-resistant cells were a much more intense green colour than the HT29 cells. This difference in intensity was clearly visible with the naked eye and was confirmed by colleagues within the lab. I wished to determine quantitatively whether or not the drug-resistant cell lines were being stained more intensely than the drug-sensitive ones. This assessment was accomplished by measuring the fluorescence of CMFDA stained cells in a pilot experiment. In this experiment, cells from each cell line were stained with CMFDA, and unstained cells were used for controls. Next, the cells were lysed to release their cellular contents and the fluorescence of the lysate solutions was measured. HCT116 and SN-38-resistant HCT116-S colon cancer cells were included as a second pair of drug-sensitive and drug-resistant cell lines to observe potential patterns across the multiple cell lines. Caco-2 colon cancer cells were included as a well-differentiated colon cancer control cell line. In observing the drug-sensitive lines, the Caco-2 cells used for CRC controls had significantly higher relative fluorescence than the HT29 and HCT116 colon cancer cells (Figure 13A). The HCT116 cells had lower levels of CMFDA conversion than the HT29 cells, as shown in Figure 13A.

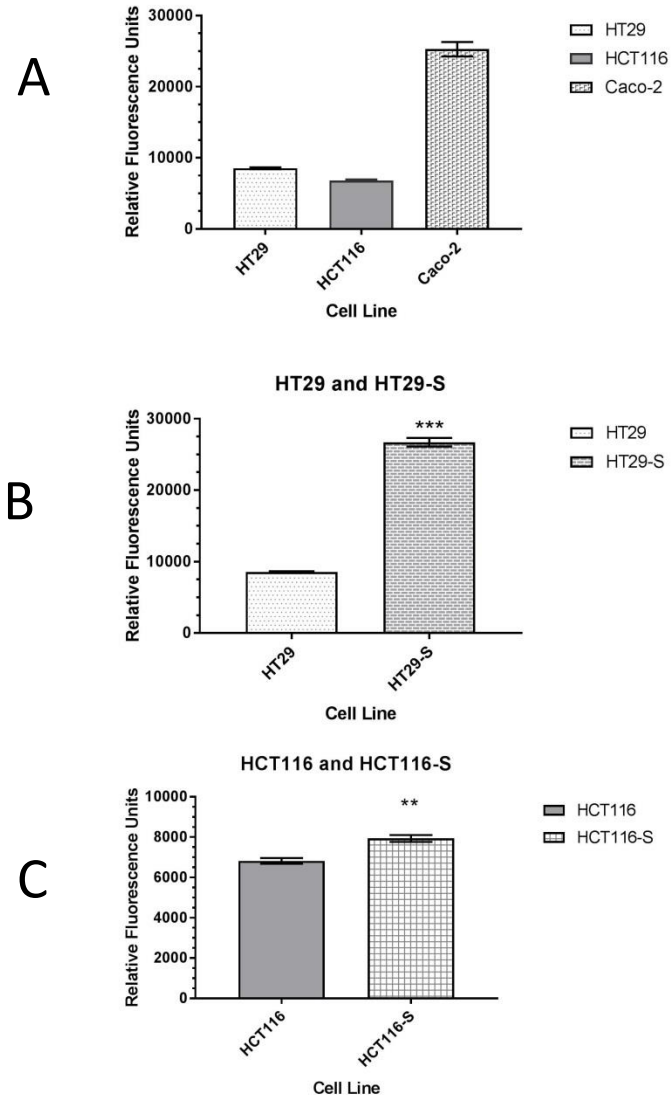

Figure 13 5-chloromethylfluorescein diacetate (CMFDA) conversion in different colon cancer cells

Relative fluorescence units of HT29 (A,B), HT29-S (B), HCT116 (A,C), HCT116-S (C), and Caco-2 (A). Three replicates of $1x10^6$ cells for each cell line were stained with 5 µL of CMFDA, and unstained cells were used as controls. Following staining, the cells were lysed with 300 µL of lysis buffer and intermittently vortexed for 30 min. After centrifugation, 200 µL of lysate supernatant was placed in a 96-well plate and the fluorescence was measured using excitation and emission wavelengths of 492 nm and 517 nm, respectively. Data were analysed with a one-way ANOVA with Bonferroni multiple comparisons test. ***$p<0.0001$ shows a highly significant increase in CMFDA conversion between HT29-S SN-38-resistant cells and HT29 SN-38-sensitive cells. ** $p=0.0002$ indicates a significant increase in CMFDA conversion between HCT116-S-SN-38 resistant cells and HCT116-SN-38 sensitive cells.

Next, CMFDA conversion was compared in the SN-38-resistant cell lines HT29-S and HCT116-S to their drug-sensitive counterparts. In both pairs, the drug-resistant cells showed higher levels of CMFDA conversion than the drug-sensitive cells. This difference was particularly notable in the HT29 and HT29-S pair as there was nearly a three-fold increase in CMFDA conversion in the HT29-S cells ($p<0.0001$), shown in Figure 13B. The difference was less dramatic in the HCT116 and HCT116-S pair ($p=0.0002$), but the HCT116-S drug-resistant cells did show marginally elevated CMFDA conversion, as shown in Figure 13C. The Caco-2 cell line exhibited extremely high levels of fluorescence, indicating extensive enzymatic conversion of the CMFDA. These high levels are likely resulting from the highly differentiated nature of the Caco-2 colon cancer cells. The fluorescent readings of all the unstained control cells were negligible. Once it was determined that there were indeed differences in the enzymatic conversion of CMFDA between the drug-resistant and drug-sensitive cell lines, further experiments could be done to elaborate on where enzyme conversion differs.

3.3 Carboxylesterase

3.3.1 4-methylumbelliferyl acetate (4-MUBA) conversion in colon cancer cells

The first assay chosen to assess CES activity was the conversion of 4-MUBA into the fluorescent product 4-methyumbelliferone. Cells were grown and lysed to release their cellular contents. The supernatant from the lysate was placed in a 96-well plate and 4-MUBA added. The fluorescence of the 4-MUBA and lysate mixes was measured after 2.5 h.

In all of the cell lines, the conversion of 4-MUBA and resulting fluorescence increased as the 4-MUBA concentration was increased. The HT29-S and HCT116-S cells had elevated levels of activity compared to the SN-38-sensitive cells (Figure 14A and Figure 14B), suggesting CES activity may be related to drug resistance. After compiling the data of four independent experiments, only the 0.2 mM concentration of 4-MUBA with HT29 and HT29-S showed any significant difference ($p=0.0018$; Figure 14A). The lack of significance in this compilation could be attributed to the inter-experimental variation in fluorescence levels, because within individual experimental data sets there were significant differences (data not shown). The compiled data are presented in Figure 14, and general trends can be seen between drug-resistant and drug-sensitive cells within pairings. Caco-2 cells exhibited high CES activity levels (Figure 14C); this is unsurprising given their highly differentiated nature.

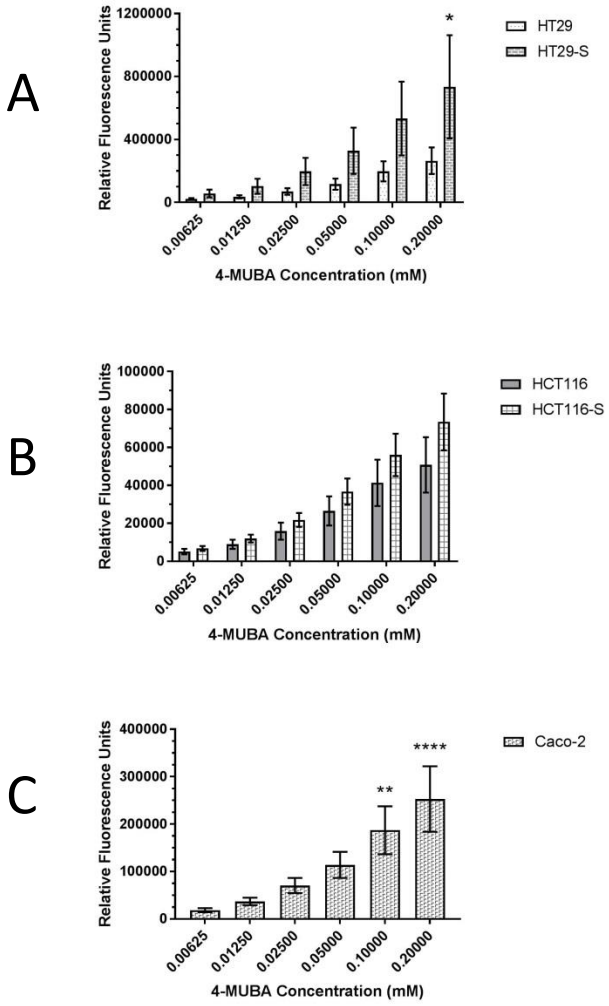

Figure 14 Carboxylesterase activity in different colon cancer cells using 4-methyumbelliferyl acetate (4-MUBA)

HT29 and HT29-S (A), HCT116 and HCT116-S (B), and Caco-2 (C) cell lines were grown to 90% confluence in 24-well plates, and were lysed with 100 µL of lysis buffer for 30 min at 4 °C. The lysate was centrifuged and 80 µL of supernatant was added to a 96-well plate prepared with six concentrations of 4-methyumbelliferyl acetate (4-MUBA). Carboxylesterase enzyme activity was assessed through conversion of 4-MUBA into the fluorescent product 4-methyumbelliferone after a 2.5 h incubation at room temperature. Excitation and emission spectra were 350 nm and 450 nm respectively. Relative fluorescence values were normalised within each experiment by subtracting the blank control values and adjusting the resulting values to cell counts for each cell line. The data are means ± SEM. All three panels show data from four independent experiments. Data were analysed with a two-way ANOVA with Bonferroni multiple comparisons test (A, B) and Dunnett's multiple comparisons test (C). *p=0.0018 shows a significant increase in carboxylesterase activity in HT29-S SN-38-resistant cells compared to HT29 drug-sensitive cells at a 4-MUBA concentration of 0.2 mM.

3.3.2 p-nitrophenyl acetate (pNP) conversion in colon cancer cells

In addition to the 4-MUBA assay, I wanted to compare with a different CES activity assay that used a colourimetric reaction. In this assay, pNP was hydrolysed by CES and converted into the yellow product p-nitrophenolate. pNP solutions were added to cells in 24-well plates and incubated for 2 hours. Supernatant was removed at 20 min, 40 min, and 120 min time intervals and the absorbance measured.

There was a drop in the absorbance values for HT29 and HCT116 cells after 120 min exposure to pNP, especially at elevated concentrations, as seen in Figure 7 and Figure 8. I determined that it would be best to use the values obtained from the 40 min interval when collecting and combining data from the multiple experiments.

While observing the absorbance values, the drug-resistant cells once again had elevated levels of CES activity, similar to the findings using 4-MUBA. There was an increase in enzymatic conversion of pNP with the increasing concentrations of pNP across all cell lines, as indicated in Figure 15. The HT29-S cells displayed elevated enzyme activity compared to the HT29 cells (Figure 15A). The HCT116-S cells exhibited higher activity than HCT116 (Figure 15B). At concentrations greater than 2 mM of pNP, there is a drop in the absorbance in HT29 and HCT116 cells. This decrease is likely related to cytotoxic effects of the pNP at high concentrations (Figure 7). The drug-resistant cells seem to be less affected by the presence of higher concentrations of pNP. Caco-2 cells exposed to the 8 mM pNP concentration had significantly higher absorbance values after 40 min when compared to the lowest 0.25 mM concentration ($p=0.0046$; Figure 15C).

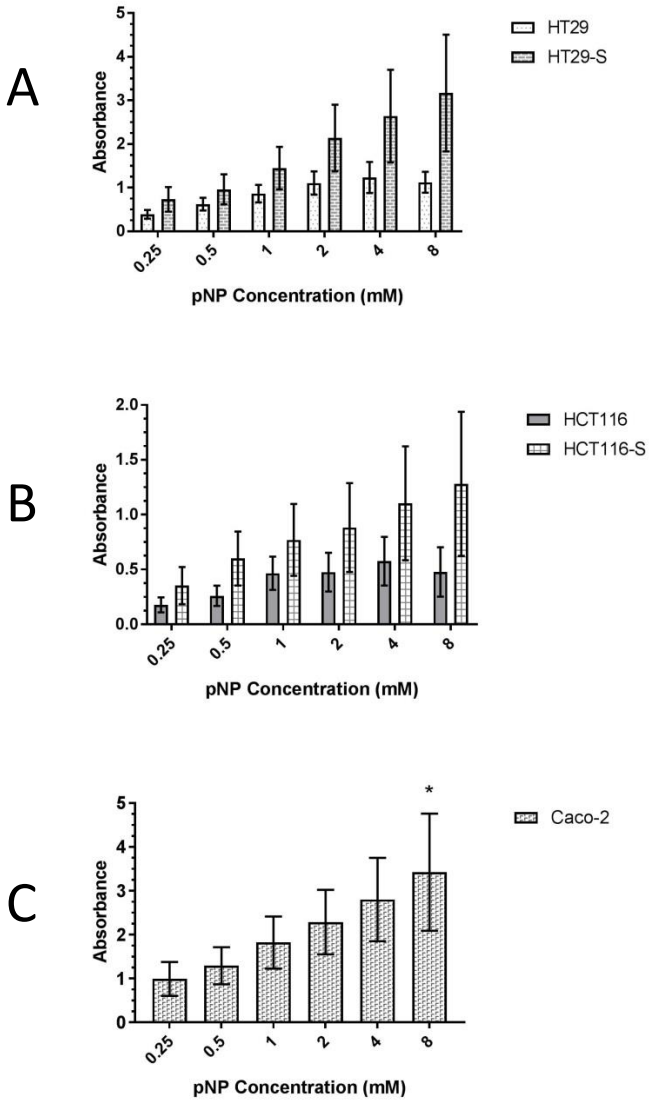

Figure 15 Carboxylesterase activity in different colon cancer cells using p-nitrophenyl acetate (pNP)

HT29 and HT29-S (A), HCT116 and HCT116-S (B), and Caco-2 (C) cell lines were grown to 90% confluence in 24-well plates. 250 µL of p-nitrophenyl acetate (pNP) solutions at six concentrations were added to the wells. Carboxylesterase activity was measured using pNP cleavage into p-nitrophenolate, a yellow-coloured product. 50 µL of supernatant was removed after 40 min, and absorbance was measured at 405 nm. Absorbance values were normalised within each experiment by subtracting the blank control values and adjusting the resulting values to cell counts for each cell line. The data are means ± SEM. All three panels show data compiled from four independent experiments. Data were analysed with a two-way ANOVA with Bonferroni multiple comparisons test (A,B) and Dunnett's multiple comparisons test (C). *p=0.0046 shows a significant increase in carboxylesterase activity in Caco-2 cells at a pNP concentration of 8 mM compared to 0.25 mM.

3.4 Glutathione S-Transferase

In addition to the enzymes that convert the CMFDA into a green fluorescent product, it was prudent to investigate GST, the enzyme that transforms CMFDA into its membrane-impermeable form. The 1-chloro-2,4-dinitrobenzene (CDNB) used is conjugated with reduced glutathione (GSH) by the GST enzyme, generating a yellow-coloured product. Elevated levels of GST activity were noted in the HT29-S cells when compared to HT29 (Figure 16A). A general trend of increasing activity as the concentrations of CDNB and GSH were raised was also present. The HCT116 and HCT116-S cells showed no distinctive patterns across concentrations or between cell lines (Figure 16B). The Caco-2 cells showed high levels of activity overall, indicating high enzymatic activity (Figure 16C).

After compiling the data from four independent experiments, I noted that GST activity in the HCT116 and HCT116-S pair did not show the same patterns of drug-resistant cells having elevated enzyme activity compared to drug-sensitive cells as was previously described in the pilot experiment (Figure 13) and CES assays (Figure 14 and Figure 15). In this instance there does not appear to be any clear trend to the data, even between the different concentrations of mixes. This indicates that GST levels are not being affected by the drug resistance in the HCT116 pair of cell lines.

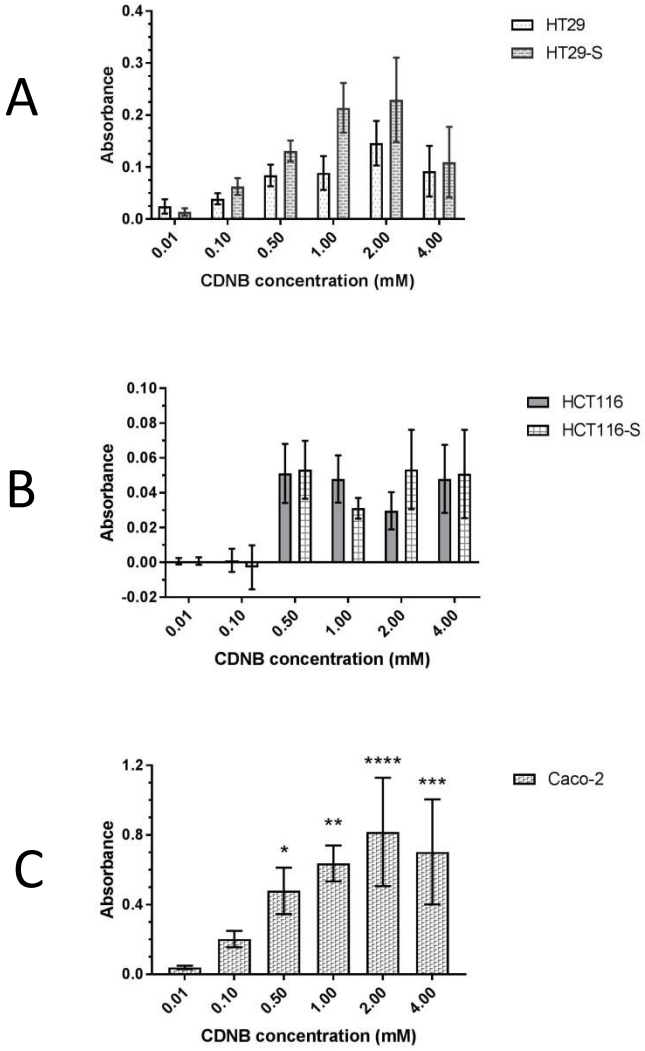

Figure 16 Glutathione S-transferase activity in different colon cancer cells using 1-chloro-2,4-dinitrobenzene (CDNB) and reduced glutathione (GSH)

HT29 and HT29-S (A), HCT116 and HCT116-S (B), and Caco-2 (C) cell lines were grown to 90% confluence in 24-well plates, and were lysed with 100 µL of lysis buffer for 2 h at room temperature. The lysates were separated using centrifugation and 20 µL of supernatant added to a 96-well plate. Six concentrations of CDNB and GSH, with ratios of 1:2, were added to the supernatant samples. GST activity was measured using the resulting yellow coloured product from the conjugation of CDNB and GSH. Absorbance was measured at 340 nm after 10 min reaction time at room temperature. Absorbance values were normalised within each experiment by subtracting the blank control values and adjusting the resulting values to cell counts for each cell line. The data are means ± SEM. All three graphs show data from four independent experiments, with no normalisation between experiments. Data were analysed with a two-way ANOVA with Bonferroni multiple comparisons test (A,B) and Dunnett's multiple comparisons test (C). *p=0.0354, **p=0.0053, ***p=0.0007, ****p<0.0001

In contrast, the HT29 and HT29-S pair exhibit a trend of increasing activity along the concentration levels, as well as elevated activity in the SN-38-resistant HT29-S cells compared to the HT29 cells (Figure 16A). There was a decrease in enzyme activity when the concentration of CDNB was 4 mM; this decrease is likely indicative of cytotoxicity from the substrate mix at higher concentrations. With the Caco-2 cells, the enzyme activity increased as the concentrations of substrate mix increased, until a 4 mM CDNB concentration was reached, at which point there was a decrease in activity (Figure 16C). The differences along the concentration changes for Caco-2 were significant at the 0.5 mM, 1.0 mM, 2.0 mM, and 4.0 mM concentrations ($p=0.035$, $p=0.0053$, $p<0.0001$, and $p<0.001$), as indicated in Figure 16.

Chapter 4. Discussion

4.1 Perspective

Drug resistance in CRC coincides with altered behaviours of the cells, leading to more aggressive phenotypes. Resistance is promoted through a variety of mechanisms including drug metabolism [26, 27]. In this project the initial intent was to investigate the cellular behaviours of drug-resistant colon cancer cells through the use of adhesion assays. However, these experiments led to the novel observation that the SN-38-resistant cells were stained more vibrantly than the SN-38-sensitive cells. To assess this observation, enzymes involved in both the metabolism of the cell stain, the metabolism of irinotecan, and drug resistance were assessed for activity levels, namely, CES and GST [22, 63, 64].

4.2 Cell Adhesion

Little, if any, binding of HT29 cells to the FN coating was observed, although adhesion increased in the context of HepG2. This increase in adhesion when comparing the HepG2 and fibronectin experiments is understandable because the ECM generated by the HepG2 cells has a wider variety of components to which the HT29 cells can adhere. The HT29 cells are not limited to only using fibronectin receptors to attach to the ECM, and can employ other cell-ECM binding proteins. The drug-resistant HT29-S cells had elevated adhesion compared to the drug-sensitive HT29 cells in both the HepG2 and fibronectin experiments.

HT29-S cells were often observed in clumps when adhered to the substratum. This cell-to-cell adhesion is likely initiated prior to the addition of the cell suspension to coated wells. This indicates that the drug-resistant cells have high levels of cell-to-cell adhesion in addition to adhesion to the ECM. Elevated adhesion has been observed in other drug-resistant cancers as well [50]. The enhanced adhesion of these cells likely contributes to pro-survival signals, such as those initiated through integrin binding [46], and is a trait that would benefit these cells when they are mobile and traveling through the body. Once the cells locate a favourable environment, they may have a greater likelihood of being able to adhere there given these findings.

During the adhesion experiments, I noticed that the drug-resistant HT29-S cells were brighter green when stained with the CMFDA than the drug-sensitive HT29 cells. It was postulated that the difference in colouration and brightness could be an optical illusion, or it could be a genuine effect. To pursue the latter idea further, cells were stained with CMFDA and the fluorescence observed (Figure 13). Included in this experiment were HCT116 and HCT116-S cells to add another pair of drug-sensitive and drug-resistant cells to observe. Caco-2 cells were used for colon cancer controls because the HepG2 cells were of liver origin. The Caco-2 cells were also well differentiated, which provided some information on cells that have more mature enzyme profile with elevated expression of particular enzymes and processes in place.

4.3 5-chloromethylfluorescein diacetate (CMFDA)

CMFDA is clear, colourless, and moves passively through cellular membranes. It is used to fluorescently label live cells to observe their morphology and behaviour. Once inside a cell, an acetate group is cleaved from the molecule by esterases, generating a green and fluorescent product (Figure 17). GSTs conjugate GSH to CMFDA, which transforms CMFDA into a membrane-impermeable form (Figure 17). CMFDA is simple to use, effective at staining, and does not harm the cells – it was selected as the stain of preference for these reasons.

While performing adhesion experiments, HT29-S cells appeared to be more brightly coloured and fluorescing than the HT29 cells. This was a repeated observation over the course of multiple experiments and was confirmed with colleagues. This continual occurrence led to deeper investigation of the stain being used, its mechanism of action, and how these might relate to drug resistance. It was suspected that the differential staining could be the result of altered CMFDA processing within the SN-38-resistant cells.

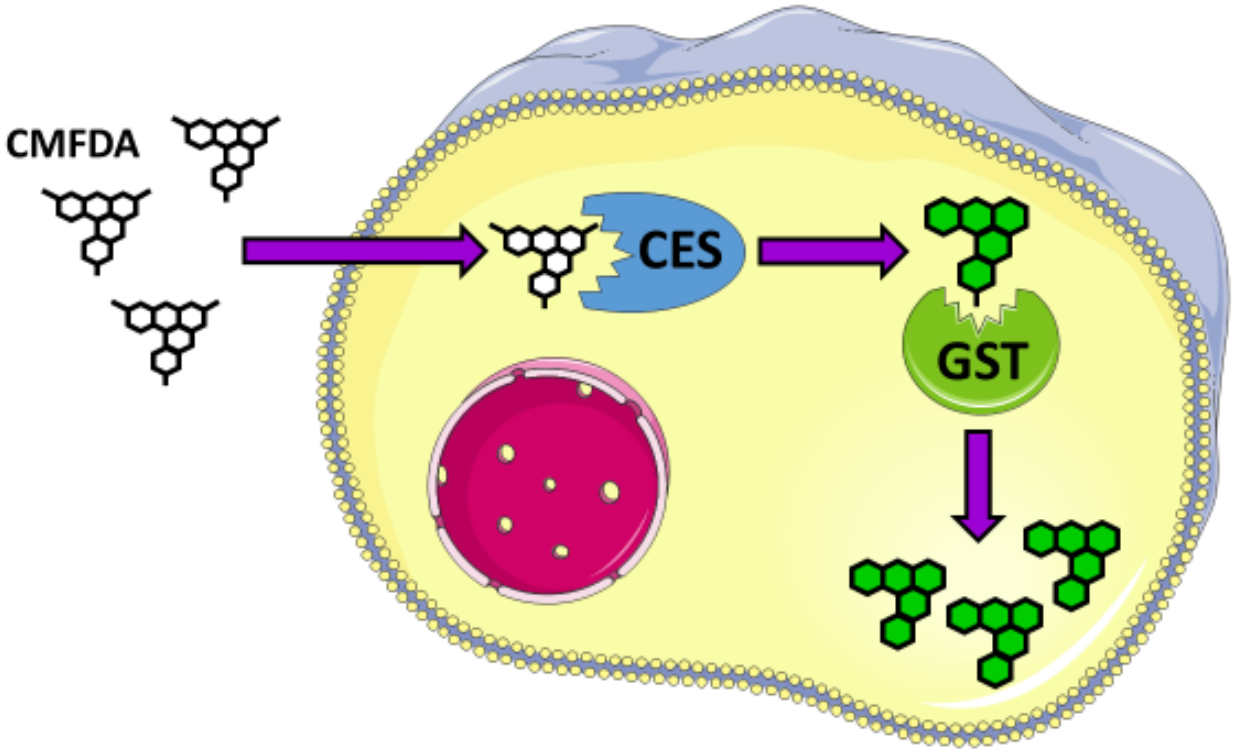

Figure 17 5-chloromethylfluorescein (CMFDA) conversion within a cell
5-chloromethylfluorescein (CMFDA) is a clear, colourless compound that is membrane permeable and moves passively into cells. Carboxylesterase (CES) converts CMFDA into a green and fluorescent product. Glutathione S-transferase (GST) changes CMFDA from a membrane permeable to a membrane-impermeable compound.

The assessment of the question – is there a difference in CMFDA conversion between drug-sensitive and drug-resistant cells – was accomplished through a simple pilot experiment involving the staining of six cell lines, two drug-resistant, their drug-sensitive counterparts, and two potential control cell lines. The different intensities of fluorescence within the cells after treatment with CMFDA (Figure 13) indicate that the enzymes responsible for processing CMFDA into its green fluorescent product are present or active in different levels. The more vibrant green indicates that the CMFDA is being converted more by CES, or there is greater retention of the product through increased GST activity.

It was determined from the pilot experiment that the investigation of enzyme activity was worth pursuing, with a focus on CES because of its involvement in both irinotecan metabolism [63] and CMFDA conversion. GST was the other enzyme selected because it is known to contribute to drug resistance [38, 61] and also converts CMFDA.

4.4 Carboxylesterase

4.4.1 Overview

There is a noticeable difference in carboxylesterase (CES) activity between drug-resistant and drug-sensitive cells as indicated in the 4-MUBA (Figure 14) and pNP (Figure 15) experiments. This difference relates to the treatment of patients with irinotecan because CES1 and CES2 are prominently involved in the metabolism of irinotecan through the generation of the active metabolite SN-38. Both extracellular metabolism at the cell surface and intracellular CES activity were assessed through these experiments. The 4-MUBA assays account for both cell membrane bound and intracellular CES [54] because cell lysates were used, whereas the pNP assays would have given a better indication of the metabolism occurring at the cell surface because whole cells rather than lysates were used.

4.4.2 4-methyumbelliferyl acetate (4-MUBA) conversion in SN-38-resistant colon cancer cells

CES activity was measured using 4-MUBA cleavage into the fluorescent product 4-methylumbelliferone. In all five cell lines, there was an increase in enzyme activity as the 4-MUBA concentration was increased (Figure 14). The HT29-S and HCT116-S SN-38-resistant cells had elevated CES activity in comparison to their SN-38-sensitive counterparts. This difference in activity was especially evident in the HT29-S cell line, and less so between the HCT116 and HCT116-S pair; these results follow the trends displayed in Figure 13. The HT29-S cells showed a roughly 3-fold increase in CMFDA conversion in the pilot experiment (Figure 13) and a 2.5- to 2.7-fold increase across the concentrations in the compiled 4-MUBA experimental data (Figure 14). The HCT116-S cells exhibited a 1.2-fold increase in the pilot experiment and the compiled data shows a range of roughly a 1.3- to 1.5-fold increase. These values between the pilot experiment and CES activity assays are similar and indicate that CES activity is likely responsible for the majority of the difference in CMFDA staining within these cell lines.

4.4.3 p-nitrophenyl acetate (pNP) conversion in SN-38-resistant colon cancer cells

Another assay used to measure CES activity was the colourimetric reaction involving pNP cleavage. This assay hinges on CES cleaving an acetate group off of pNP to generate p-nitrophenolate which is a yellow-coloured product. This reaction can also occur passively depending of the pH of the solution used; a pH of 7.0 was used in these experiments to prevent dissociation.

The drug-resistant cell lines HT29-S and HCT116-S showed elevated levels of CES activity (Figure 15) and had values consistent with those from the 4-MUBA experiments and the CMFDA pilot experiment. Interestingly, the drug-resistant cells were less affected by the presence of higher concentrations of pNP and did not experience as much cytotoxicity as the drug-sensitive cell lines. This is indicative of a pro-survival mechanism that would prevent the cells from dying, although may not be directly linked to how the cells respond to pNP. Rather, the drug-resistant cells may have alternative survival mechanisms employed, such as evasion of apoptosis or altered cell signalling, to prevent cell death [26]. There was no decrease in cell viability noticed in the Caco-2 cells.

4.4.4 Importance of carboxylesterase activity in drug resistance

How might these results contribute to our understanding of where the resistance of these cells is occurring? In regards to the metabolism of irinotecan, elevated levels of CES in the intestinal cells would not play much of a role until second pass metabolism of the drug. Irinotecan is administered intravenously and the primary metabolism of irinotecan would be occurring in the liver, which has high levels of CES [65]. The inactive metabolite of irinotecan, SN-38G, is secreted into the bile, which then enters the digestive tract. Once in the tract, bacteria can cleave the SN-38G and reform the active metabolite SN-38 [22]. Although this processing of SN-38G would expose the CRC to the more potent metabolite of irinotecan, it does not explain the elevated CES in the CRC. Elevated CES could convert any irinotecan that passes through the liver and eventually perfuses the CRC cells [66].

In the context of these *in vitro* assays, an alteration to the metabolic pathway elsewhere in the cells is more likely occurring. The final product of CES conversion of irinotecan is already present, and so the enzymes become of little consequence in regards to conversion. This would mean that the cells are likely responding to the SN-38 exposure in different ways. It is possible that elevated levels of CES2 are in fact a secondary occurrence that could be the result of other treatments or additional aberrations that may be present within the cells, for example the regulation of CES2 by p53 [67].

4.4.5 Clinical relevance of carboxylesterase in colorectal cancer

CES expression levels could play a role in clinical outcomes. Elevated levels of CES2 in primary tumours may be indicative of more aggressive phenotype [68]. In the context of a patient, the CRC might have elevated CES levels as a result 5-FU being present within the treatment regimen. 5-FU can induce CES2 expression and protein levels within CRC [67], and given that patients with metastatic CRC are treated with a combination of irinotecan, 5-FU, and leucovorin [11], it may not be as simple as elevated CES2 being directly linked to tumour aggressiveness. Although other forms of CES do exist within colon tissue, CES2 is the most abundant and active in regards to irinotecan hydrolysis [69]. In other cancers, such as pancreatic ductal adenocarcinoma, elevated CES2 expression corresponds with better survival when treated with irinotecan [70]. Given this information, it is possible that similar implications for survival may exist for some patients with CRC.

4.5 Glutathione S-Transferase

4.5.1 Overview

GST has been implicated in drug resistance [71], and also converts CMFDA into a membrane-impermeable form. When this information is considered in conjunction with the results from the CMFDA conversion pilot experiment (Figure 13) it becomes apparent that GST may have some involvement in the drug resistance processes of the HT29-S and HCT116-S cells. This possibility was further tested by performing GST enzyme activity assays with five colon cancer cells lines – HT29, HT29-S, HCT116, HCT116-S, and Caco-2.

Through these experiments, HCT116 and HCT116-S cells showed no distinctive patterns or trends between the cell lines or across the different substrate concentrations (Figure 16). This likely indicates the GST is not playing a significant role in the drug-resistance mechanisms found within the HCT116-S cells. These particular results also indicate that the differences in CMFDA conversion found within the HCT116 and HCT116-S cells (Figure 13) are not necessarily explained by an increase in GST activity. The fluctuations in GST activity levels shown in Figure 16 may be explained by where in the cell cycle the majority of cells were at the time of the experiments. GST is known to be present at higher levels in growing cells, but lower levels in differentiating and maturing cells [59]. The Caco-2 cell line displayed a general trend of increasing activity as the concentrations of the substrates were increased. This trend is indicative of a consistent level of functioning GST and substrate concentrations that do not fully saturate the enzyme.

Of particular interest in the GST activity assays were the HT29 and HT29-S pair of cell lines. The HT29-S cells exhibited higher levels of GST activity than their drug-sensitive counterparts. GST is likely contributing to the drug resistance of the HT29-S cells, and in the very least aids in retention of the CMFDA stain. The alteration in GST activity could possibly be explained by upregulation of the enzyme, however, further testing of gene expression and protein levels would be necessary to confirm this.

4.5.2 Glutathione S-transferase involvement in cell survival

The elevated levels of GST in SN-38-resistant HT29-S cells bring to question whether or not GST is directly involved in resistance mechanisms. In all likelihood, GST does not directly contribute to the drug-resistance of these cells, but rather contributes to their ability to survive and thrive in conditions that would otherwise stimulate apoptosis. In essence, elevated GST acts in a pro-survival manner. This is quite likely given some findings that GST is not in and of itself causing drug resistance, but may be elevated in response to the exposure of SN-38 [60]. In order to confirm this, further assays would need to be performed involving the specific inhibition of GST to determine if cells become sensitised to the presence of SN-38.

GSTP exists in a monomeric and dimeric state (Figure 18). The dimeric state is primarily responsible for the conversion of substrates. In the monomeric state, GSTP binds to JNK and functionally inhibits it [61], thereby preventing downstream signalling from JNK to Bax and other pro-apoptotic Bcl2-family proteins [62, 72, 73]. GSTP enables cell survival through the inhibition of pro-apoptotic signalling cascades initiated by JNK1. By improving survival capabilities of the cells, the cells have a greater opportunity to acquire drug resistance through alternative mechanisms, such as those shown in Figure 4. HT29-S cells had significantly higher levels of GST activity compared to HT29 cells (Figure 16). These elevated levels of GST could be contributing to a reduction in the pro-apoptotic signals that are transduced via JNK signalling.

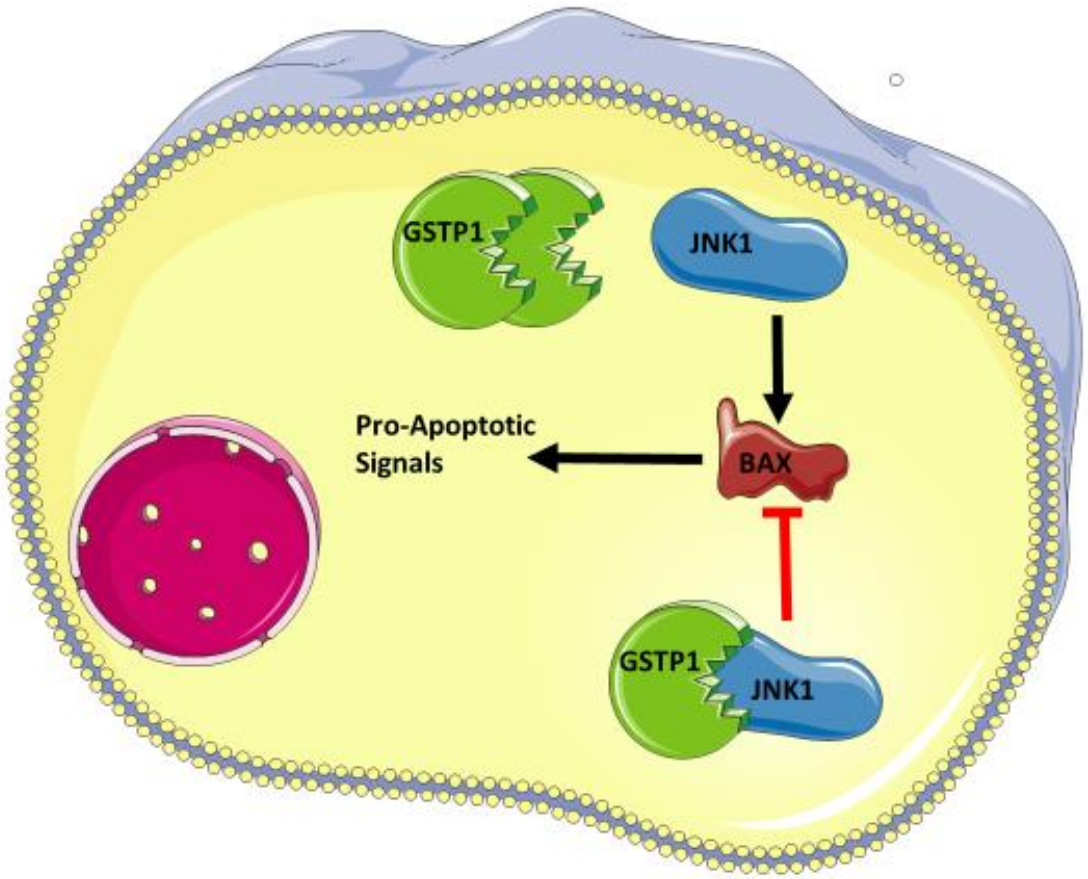

Figure 18 GSTP1 inhibition of JNK1

Dimeric GSTP1 acts primarily to conjugate reduced glutathione to xenobiotics to facilitate their removal, and does not bind to JNK1. This allows JNK1 to signal the Bcl-2 family protein Bax which in turn promotes pro-apoptotic signaling. Monomeric GSTP1 forms a protein complex with JNK1, which inhibits the signaling capacity of JNK1 and ensuing pro-apoptotic signal cascade through Bax.

Additionally, JNK signalling pathways were recently highlighted as important apoptotic pathways in KRAS-mutant CRC cells, and these pathways can be induced through flavonoids such as quercetin [74]. Another example of overcoming drug resistance through JNK activation involved the addition of thymoquinone to irinotecan-resistant metastatic colon cancer cells [75]. Although GSTP may be involved in cell survival and apoptotic pathways, there are many ways in which these pathways can be altered. For example, in irinotecan-resistant cells, GSTP was elevated along with RhoA; when RhoA activity was reduced through the use of siRNA, the cancer cells regained some sensitivity to irinotecan [76]. This highlights the complexity of the involvement of apoptotic pathways and GSTP within them. It is quite possible that even if one avenue of resistance is being treated, these cells may have alternative resistance mechanisms or pathways through which survival or apoptotic signals can be altered to improve the survivability of the cells.

4.5.3 Clinical considerations of glutathione S-transferase in cancer treatment

In regards to clinical considerations of GST activity, the treatment of cells with GST inhibitors is a potential avenue for cancer treatment. This would play into the dual nature of GST as a detoxifying enzyme, as well as its role in the reduction of pro-apoptotic signalling. If GSTP activity were reduced this would, in theory, open up the pro-apoptotic signalling cascade mediated by JNK, and there would also be a reduction in GSTP mediated inactivation of xenobiotics and treatments. Additionally, GSTP could be used to activate pro-drugs, which would then potentially target cancer cells with elevated levels of this enzyme [77]. In considering this route, it would be important to assess the balance of monomeric and dimeric GSTP because the ratio could potentially affect whether the GSTP protein is acting in an enzymatic conversion capacity or as a complexing protein to alter apoptotic signalling within the cells. In addition to GST activity, genetic polymorphisms in GST genes may be of interest when considering clinical decisions. For example, progression free survival outcomes for patients with metastatic CRC and treated with irinotecan were better in patients with a specific GSTP1 polymorphism [78].

4.6 Limitations of this Work

One of the primary limitations inherent in this work is that it is *in vitro*. There is the distinct possibility that this *in vitro* work will not fully transfer or have similar results *in vivo*, which is unfortunately a common issue that arises in biological studies and the path of bench to bedside. The inclusion of other cell lines – such as the SW480 and SW620 pair that originate from the same patient – may have shed light onto a more natural acquisition of resistance. Primary patient isolates would have also provided an opportunity to improve and expand this work.

Additionally, there is a lack of expression data within this study that could have been acquired through PCR-based experiments. As well, western blots could be used to observe changes in the levels of the proteins of interest, namely CES2 and GSTP1. These tests would add additional information regarding the gene expression and presence of a more mature enzyme profile, which would clarify where in the generation and processing the enzymes are being affected and potentially changed. This merits further investigation.

Within the experiments performed, the possibility exists that other enzymes may be capable of cleaving 4-MUBA and pNP. This could have been addressed in part through information obtained from protein expression assays such as Western blots to assess the presence of other CES enzymes. Spontaneous conversion of these substrates was addressed by using blanks exposed to the same conditions as the rest of the assay. In hindsight, the CES activity assays are not as similar as could have been. The pNP assay mainly addresses cell surface CES that converts the substrate, whereas the 4-MUBA assay addresses all CES, intracellular and extracellular, because of the use of lysates.

4.7 Significance of this Work

The work done in this study adds to existing literature regarding the implications of particular enzymes in drug resistance, specifically how CES and GSTP may be involved in resistance and pro-survival mechanisms. This study highlights how enzymes may be involved in perpetuating drug resistance. Through this work, I was able to gain more insight into where in the chain of events drug resistance may be evolving within the HT29-S and HCT116-S cell lines developed by the Blay lab.

Additionally, the complexity and interaction of treatments is brought to the forefront of discussion in regards to treating late stage and metastatic disease. It is quite likely that although somewhat effective, combination therapies may also be eliciting synergistic or combating responses. One example of this is highlighted by the variations that can be found in CES activity and its importance in the irinotecan metabolic pathway. This work also contributes to understanding of how CES and GST may have further implications in clinical outcomes.

References

1. Fearon, E.R. and B. Vogelstein, *A genetic model for colorectal tumorigenesis.* Cell, 1990. **61**(5): p. 759-67.
2. Vogelstein, B., et al., *Genetic alterations during colorectal-tumor development.* N Engl J Med, 1988. **319**(9): p. 525-32.
3. Gryfe, R., et al., *Molecular biology of colorectal cancer.* Curr Probl Cancer, 1997. **21**(5): p. 233-300.
4. Sansom, O.J., et al., *Loss of Apc in vivo immediately perturbs Wnt signaling, differentiation, and migration.* Genes Dev, 2004. **18**(12): p. 1385-90.
5. Baker, S.J., et al., *Chromosome 17 deletions and p53 gene mutations in colorectal carcinomas.* Science, 1989. **244**(4901): p. 217-21.
6. Jung, B., J.J. Staudacher, and D. Beauchamp, *Transforming Growth Factor beta Superfamily Signaling in Development of Colorectal Cancer.* Gastroenterology, 2017. **152**(1): p. 36-52.
7. Risio, M., et al., *Deletions of 17p are associated with transition from early to advanced colorectal cancer.* Cancer Genet Cytogenet, 2003. **147**(1): p. 44-9.
8. Johns, L.E. and R.S. Houlston, *A systematic review and meta-analysis of familial colorectal cancer risk.* Am J Gastroenterol, 2001. **96**(10): p. 2992-3003.
9. Huels, D.J. and O.J. Sansom, *Stem vs non-stem cell origin of colorectal cancer.* Br J Cancer, 2015. **113**(1): p. 1-5.
10. Siegel, R., C. Desantis, and A. Jemal, *Colorectal cancer statistics, 2014.* CA Cancer J Clin, 2014. **64**(2): p. 104-17.
11. Network, N.C.C. *Clinical Practice Guidelines in Oncology (NCCN Guidelines) Colon Cancer Version 3.2013*. 2012.
12. Kemeny, N., *Management of liver metastases from colorectal cancer.* Oncology (Williston Park), 2006. **20**(10): p. 1161-76, 1179; discussion 1179-80, 1185-6.
13. Eveno, C., et al., *Proof of prometastatic niche induction by hepatic stellate cells.* J Surg Res, 2015. **194**(2): p. 496-504.
14. Pelillo, C., et al., *Colorectal Cancer Metastases Settle in the Hepatic Microenvironment Through alpha5beta1 Integrin.* J Cell Biochem, 2015. **116**(10): p. 2385-96.
15. Derouet, M., et al., *Acquisition of anoikis resistance promotes the emergence of oncogenic K-ras mutations in colorectal cancer cells and stimulates their tumorigenicity in vivo.* Neoplasia, 2007. **9**(7): p. 536-45.
16. Douillard, J.Y., et al., *Irinotecan combined with fluorouracil compared with fluorouracil alone as first-line treatment for metastatic colorectal cancer: a multicentre randomised trial.* Lancet, 2000. **355**(9209): p. 1041-7.
17. Longley, D.B., D.P. Harkin, and P.G. Johnston, *5-fluorouracil: mechanisms of action and clinical strategies.* Nat Rev Cancer, 2003. **3**(5): p. 330-8.
18. Rampazzo, C., et al., *Regulation by degradation, a cellular defense against deoxyribonucleotide pool imbalances.* Mutat Res, 2010. **703**(1): p. 2-10.
19. Covey, J.M., et al., *Protein-linked DNA strand breaks induced in mammalian cells by camptothecin, an inhibitor of topoisomerase I.* Cancer Res, 1989. **49**(18): p. 5016-22.
20. Kawato, Y., et al., *Intracellular roles of SN-38, a metabolite of the camptothecin derivative CPT-11, in the antitumor effect of CPT-11.* Cancer Res, 1991. **51**(16): p. 4187-91.
21. Smith, N.F., W.D. Figg, and A. Sparreboom, *Pharmacogenetics of irinotecan metabolism and transport: an update.* Toxicol In Vitro, 2006. **20**(2): p. 163-75.
22. Mathijssen, R.H., et al., *Clinical pharmacokinetics and metabolism of irinotecan (CPT-11).* Clin Cancer Res, 2001. **7**(8): p. 2182-94.

23. Gelderblom, H.A., et al., *Oral topoisomerase 1 inhibitors in adult patients: present and future.* Invest New Drugs, 1999. **17**(4): p. 401-15.
24. Burke, T.G., et al., *The important role of albumin in determining the relative human blood stabilities of the camptothecin anticancer drugs.* J Pharm Sci, 1995. **84**(4): p. 518-9.
25. Shargel, L., S. Wu-Pong, and A.B.C. Yu, *Chapter 7. Pharmacokinetics of Oral Absorption*, in *Applied Biopharmaceutics & Pharmacokinetics, 6e*. 2012, The McGraw-Hill Companies: New York, NY.
26. Gottesman, M.M., *Mechanisms of cancer drug resistance.* Annu Rev Med, 2002. **53**: p. 615-27.
27. Gottesman, M.M., et al., *Toward a Better Understanding of the Complexity of Cancer Drug Resistance.* Annu Rev Pharmacol Toxicol, 2016. **56**: p. 85-102.
28. Longley, D.B. and P.G. Johnston, *Molecular mechanisms of drug resistance.* J Pathol, 2005. **205**(2): p. 275-92.
29. Swanton, C., *Intratumor heterogeneity: evolution through space and time.* Cancer Res, 2012. **72**(19): p. 4875-82.
30. Burrell, R.A. and C. Swanton, *Tumour heterogeneity and the evolution of polyclonal drug resistance.* Mol Oncol, 2014. **8**(6): p. 1095-111.
31. Russo, M., et al., *Tumor Heterogeneity and Lesion-Specific Response to Targeted Therapy in Colorectal Cancer.* Cancer Discov, 2016. **6**(2): p. 147-53.
32. Zanger, U.M. and M. Schwab, *Cytochrome P450 enzymes in drug metabolism: regulation of gene expression, enzyme activities, and impact of genetic variation.* Pharmacol Ther, 2013. **138**(1): p. 103-41.
33. Okon, I.S., et al., *Gefitinib-mediated reactive oxygen specie (ROS) instigates mitochondrial dysfunction and drug resistance in lung cancer cells.* J Biol Chem, 2015. **290**(14): p. 9101-10.
34. Rauch, N., et al., *MAPK kinase signalling dynamics regulate cell fate decisions and drug resistance.* Curr Opin Struct Biol, 2016. **41**: p. 151-158.
35. Shi, H., et al., *Lapatinib resistance in HER2+ cancers: latest findings and new concepts on molecular mechanisms.* Tumour Biol, 2016.
36. Martin, A.P., et al., *Inhibition of MCL-1 enhances lapatinib toxicity and overcomes lapatinib resistance via BAK-dependent autophagy.* Cancer Biol Ther, 2009. **8**(21): p. 2084-96.
37. Li, W., et al., *Overcoming ABC transporter-mediated multidrug resistance: Molecular mechanisms and novel therapeutic drug strategies.* Drug Resist Updat, 2016. **27**: p. 14-29.
38. Harbottle, A., et al., *Role of glutathione S-transferase P1, P-glycoprotein and multidrug resistance-associated protein 1 in acquired doxorubicin resistance.* Int J Cancer, 2001. **92**(6): p. 777-83.
39. Gottesman, M.M., T. Fojo, and S.E. Bates, *Multidrug resistance in cancer: role of ATP-dependent transporters.* Nat Rev Cancer, 2002. **2**(1): p. 48-58.
40. Dessein, A.F., et al., *Autocrine induction of invasive and metastatic phenotypes by the MIF-CXCR4 axis in drug-resistant human colon cancer cells.* Cancer Res, 2010. **70**(11): p. 4644-54.
41. Kim, J.J., et al., *Acquisition of paclitaxel resistance is associated with a more aggressive and invasive phenotype in prostate cancer.* J Cell Biochem, 2013. **114**(6): p. 1286-93.
42. Lee, T.Y., et al., *Increased chemoresistance via Snail-Raf kinase inhibitor protein signaling in colorectal cancer in response to a nicotine derivative.* Oncotarget, 2016. **7**(17): p. 23512-20.
43. Kalluri, R. and R.A. Weinberg, *The basics of epithelial-mesenchymal transition.* J Clin Invest, 2009. **119**(6): p. 1420-8.
44. Chen, X., et al., *Loss of E-cadherin promotes the growth, invasion and drug resistance of colorectal cancer cells and is associated with liver metastasis.* Mol Biol Rep, 2012. **39**(6): p. 6707-14.
45. Dallas, N.A., et al., *Chemoresistant colorectal cancer cells, the cancer stem cell phenotype, and increased sensitivity to insulin-like growth factor-I receptor inhibition.* Cancer Res, 2009. **69**(5): p. 1951-7.

46. Loffek, S., C.W. Franzke, and I. Helfrich, *Tension in Cancer.* International Journal of Molecular Sciences, 2016. **17**(11).
47. Schwarzbauer, J.E. and D.W. DeSimone, *Fibronectins, their fibrillogenesis, and in vivo functions.* Cold Spring Harb Perspect Biol, 2011. **3**(7).
48. Maric, G., et al., *GPNMB cooperates with neuropilin-1 to promote mammary tumor growth and engages integrin alpha5beta1 for efficient breast cancer metastasis.* Oncogene, 2015. **34**(43): p. 5494-504.
49. Bartolome, R.A., et al., *VE-cadherin RGD motifs promote metastasis and constitute a potential therapeutic target in melanoma and breast cancers.* Oncotarget, 2016.
50. Sun, L., et al., *MGr1-Ag/37LRP induces cell adhesion-mediated drug resistance through FAK/PI3K and MAPK pathway in gastric cancer.* Cancer Sci, 2014. **105**(6): p. 651-9.
51. Damiano, J.S., et al., *Cell adhesion mediated drug resistance (CAM-DR): role of integrins and resistance to apoptosis in human myeloma cell lines.* Blood, 1999. **93**(5): p. 1658-67.
52. Gao, H., et al., *Relationships of MMP-9, E-cadherin, and VEGF expression with clinicopathological features and response to chemosensitivity in gastric cancer.* Tumour Biol, 2017. **39**(5): p. 1010428317698368.
53. Ma, S., et al., *Oridonin effectively reverses cisplatin drug resistance in human ovarian cancer cells via induction of cell apoptosis and inhibition of matrix metalloproteinase expression.* Mol Med Rep, 2016. **13**(4): p. 3342-8.
54. Schwer, H., et al., *Molecular cloning and characterization of a novel putative carboxylesterase, present in human intestine and liver.* Biochem Biophys Res Commun, 1997. **233**(1): p. 117-20.
55. Wu, M.H., et al., *Irinotecan activation by human carboxylesterases in colorectal adenocarcinoma cells.* Clin Cancer Res, 2002. **8**(8): p. 2696-700.
56. Pindel, E.V., et al., *Purification and cloning of a broad substrate specificity human liver carboxylesterase that catalyzes the hydrolysis of cocaine and heroin.* J Biol Chem, 1997. **272**(23): p. 14769-75.
57. Slatter, J.G., et al., *Bioactivation of the anticancer agent CPT-11 to SN-38 by human hepatic microsomal carboxylesterases and the in vitro assessment of potential drug interactions.* Drug Metab Dispos, 1997. **25**(10): p. 1157-64.
58. Kim, K.A., et al., *Identification of cytochrome P450 isoforms involved in the metabolism of loperamide in human liver microsomes.* Eur J Clin Pharmacol, 2004. **60**(8): p. 575-81.
59. Awasthi, S., et al., *Interactions of glutathione S-transferase-pi with ethacrynic acid and its glutathione conjugate.* Biochim Biophys Acta, 1993. **1164**(2): p. 173-8.
60. Goto, S., et al., *Significance of nuclear glutathione S-transferase pi in resistance to anti-cancer drugs.* Jpn J Cancer Res, 2002. **93**(9): p. 1047-56.
61. Townsend, D.M., et al., *Novel role for glutathione S-transferase pi. Regulator of protein S-Glutathionylation following oxidative and nitrosative stress.* J Biol Chem, 2009. **284**(1): p. 436-45.
62. Okamura, T., et al., *Phosphorylation of Glutathione S-Transferase P1 (GSTP1) by Epidermal Growth Factor Receptor (EGFR) Promotes Formation of the GSTP1-c-Jun N-terminal kinase (JNK) Complex and Suppresses JNK Downstream Signaling and Apoptosis in Brain Tumor Cells.* J Biol Chem, 2015. **290**(52): p. 30866-78.
63. Rivory, L.P., et al., *Conversion of irinotecan (CPT-11) to its active metabolite, 7-ethyl-10-hydroxycamptothecin (SN-38), by human liver carboxylesterase.* Biochem Pharmacol, 1996. **52**(7): p. 1103-11.
64. Zarate, R., et al., *Oxaliplatin, irinotecan and capecitabine as first-line therapy in metastatic colorectal cancer (mCRC): a dose-finding study and pharmacogenomic analysis.* Br J Cancer, 2010. **102**(6): p. 987-94.
65. Ross, M.K. and A. Borazjani, *Enzymatic activity of human carboxylesterases.* Curr Protoc Toxicol, 2007. **Chapter 4**: p. Unit 4 24.

66. Slatter, J.G., et al., *Pharmacokinetics, metabolism, and excretion of irinotecan (CPT-11) following I.V. infusion of [(14)C]CPT-11 in cancer patients.* Drug Metab Dispos, 2000. **28**(4): p. 423-33.
67. Xiao, D., et al., *Regulation of carboxylesterase-2 expression by p53 family proteins and enhanced anti-cancer activities among 5-fluorouracil, irinotecan and doxazolidine prodrug.* Br J Pharmacol, 2013. **168**(8): p. 1989-99.
68. Silvestris, N., et al., *CES2, ABCG2, TS and Topo-I primary and synchronous metastasis expression and clinical outcome in metastatic colorectal cancer patients treated with first-line FOLFIRI regimen.* Int J Mol Sci, 2014. **15**(9): p. 15767-77.
69. Sanghani, S.P., et al., *Carboxylesterases expressed in human colon tumor tissue and their role in CPT-11 hydrolysis.* Clin Cancer Res, 2003. **9**(13): p. 4983-91.
70. Capello, M., et al., *Carboxylesterase 2 as a Determinant of Response to Irinotecan and Neoadjuvant FOLFIRINOX Therapy in Pancreatic Ductal Adenocarcinoma.* J Natl Cancer Inst, 2015. **107**(8).
71. Kalinina, E.V., et al., *Expression of genes of glutathione transferase isoforms GSTP1-1, GSTA4-4, and GSTK1-1 in tumor cells during the formation of drug resistance to cisplatin.* Bull Exp Biol Med, 2012. **154**(1): p. 64-7.
72. Lin, C.Y., et al., *Inhibition of JNK by pi class of glutathione S-transferase through PKA/CREB pathway is associated with carnosic acid protection against 6-hydroxydopamine-induced apoptosis.* Food Chem Toxicol, 2017. **103**: p. 194-202.
73. Townsend, D.M. and K.D. Tew, *The role of glutathione-S-transferase in anti-cancer drug resistance.* Oncogene, 2003. **22**(47): p. 7369-75.
74. Yang, Y., et al., *Quercetin preferentially induces apoptosis in KRAS-mutant colorectal cancer cells via JNK signaling pathways.* Cell Biol Int, 2018.
75. Chen, M.C., et al., *Inhibition of NF-kappaB and metastasis in irinotecan (CPT-11)-resistant LoVo colon cancer cells by thymoquinone via JNK and p38.* Environ Toxicol, 2017. **32**(2): p. 669-678.
76. Ruihua, H., et al., *RhoA regulates resistance to irinotecan by regulating membrane transporter and apoptosis signaling in colorectal cancer.* Oncotarget, 2016. **7**(52): p. 87136-87146.
77. Allocati, N., et al., *Glutathione transferases: substrates, inihibitors and pro-drugs in cancer and neurodegenerative diseases.* Oncogenesis, 2018. **7**(1): p. 8.
78. Kweekel, D.M., et al., *GSTP1 Ile105Val polymorphism correlates with progression-free survival in MCRC patients treated with or without irinotecan: a study of the Dutch Colorectal Cancer Group.* Br J Cancer, 2008. **99**(8): p. 1316-21.

Appendix

A.1 Buffer and Reagent Recipes

A.1.1 Phosphate Buffered Saline

PBS (1 L, pH 7.4)
137 mM NaCl
2.7 mM KCl
10.1 mM Na_2HPO_4
1.8 mM KH_2PO_4
1 L MilliQ H_2O

A.1.2 Paraformaldehyde

3.7% PFA (pH 7.0, 10 mL prepared fresh on day of use)
370 mg PFA dissolved into 9 ml MilliQ H_2O. Use a hot plate set to low heat, stir gently with a magnetic stir bar
Add 20 µL of 5 N NaOH to assist in solubilisation.
Add 1 mL of 10X PBS.
Adjust pH to 7.0 with 20 µL of 5 N HCl.
Filter sterilize with a 0.22 µM pore filter. Keep at 37 °C prior to fixation.

A.1.3 Lysis Buffer

(pH 7.4, adjust pH before Triton X-100 addition, store at 4 °C)
50 mM Tris-HCl
2% Triton X-100
5 mM EDTA
0.25 mM NaCl

A.1.4 Phosphate Buffer with Ca^{2+} Mg^{2+}

KPBS Ca^{2+}/Mg^{2+} (1 L, pH 7.4)
90 mM KH_2PO_4
40 mM KCl
0.9 mM $CaCl_2$-$2H_2O$
0.5 mM $MgCl_2$-$6H_2O$